N-62-4-6

SPACE POWER AND PROPULSION SECTION

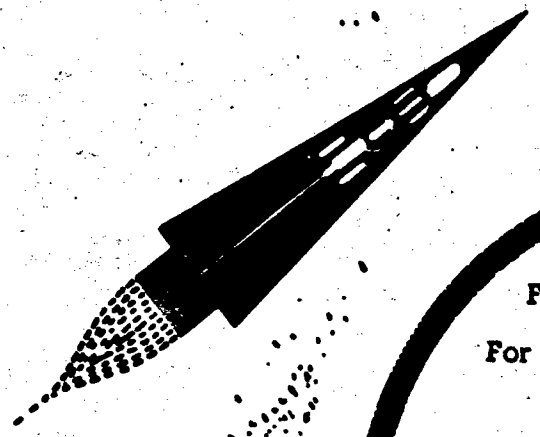

FIRST QUARTERLY REPORT

For Period Ending July 15, 1962

DYNAMIC SHAFT SEALS IN SPACE
Under Contract #AF33(657)-8459

For

Aeronautical Systems Division
Wright Patterson Air Force Base, Ohio

GENERAL ELECTRIC
CINCINNATI 15, OHIO

SPACE POWER AND PROPULSION SECTION

QUARTERLY PROJECT STATUS REPORT

JULY 15, 1962

DYNAMIC SHAFT SEALS IN SPACE

Under Contract #AF33(657)-8459

SPACECRAFT DEPARTMENT
MISSILE AND SPACE DIVISION
GENERAL ELECTRIC COMPANY
CINCINNATI 15, OHIO

TABLE OF CONTENTS

LIST OF FIGURES

I. SUMMARY

The Space Power and Propulsion Section of the General Electric Company has been under contract to the Aeronautical Systems Division, Wright Patterson Air Force Base, Ohio, since April 15, 1962, for the development of dynamic shaft seals for space applications. The objective of this program is to acquire the techniques for sealing high speed rotating shafts under the operating conditions of high temperature liquid metals and vapors, the near-vacuum environments of space, and to provide long seal life.

A. The contract specifies the following requirements:

1. The fluid to be sealed shall be potassium.
2. The seals shall be operative at fluid temperatures from the melting point of the fluid selected to 1400°F.
3. The pressure on the fluid side of the seal shall be 15 psi and the external pressure shall be 10^{-6} mm Hg.
4. The speed of the rotating shaft shall be a maximum of 36,000 rpm.
5. The seal, or seal combinations, shall be designed for 10,000 hours of maintenance-free life.
6. The working fluid, potassium, shall be used as the seal lubricant.
7. The seal, or seal combinations, shall be capable of maintaining zero leakage - in the technical sense - under all conditions of operation.

8. The seals shall be designed for a 1.0 inch diameter shaft.

9. The seals shall be capable of operating in a zero "g" environment.

B. The seal evaluation shall consist of:

1. Preliminary experiments with water.

2. 100-hour operational screening test with liquid metal.

3. Thermal-cycling test with liquid metal.

4. 3000-hour life test with liquid metal.

On April 19, 1962, a meeting was held with ASD Headquarters representatives to get the program started and to reach agreement on detail specifications. ASD agreed to consider 36,000 rpm as the maximum rpm to be used on this program. ASD approved of our overall design approach stressing the employment of non-contacting rotating fluid ring seals, also called slinger seals. ASD shared our own conviction in regard to the unsuitability of face seals to attain 10,000 hour life under the conditions specified. In regard to minimum temperature level for the liquid metal in these seals, ASD suggested - from a SPUR systems standpoint - to consider 1000°R as a minimum temperature limit. Space Power and Propulsion Section would prefer to include lower temperature levels such as 700 or 800°R in the experimental program, in order to obtain basic data over a sufficiently wide range of temperatures permitting a sound selection of seal temperature level

from a systems standpoint later. Agreement was reached not to include the electromagnetic seal in this program which appears to be a development in itself and not too promising for space turbomachinery. Design effort will be directed toward development of slinger seals without any vanes or grooving and toward screw seals. Although this approach will not deliver optimum performance it will minimize cavitation and erosion problems.

The Space Power and Propulsion Section in Evendale and the General Engineering Laboratory in Schenectady, New York, will be partners in this program. This partnership is strictly an internal General Electric arrangement with the purpose of making more experience, manpower and test facilities available to this program. SPPS will be responsible for the overall program, GEL will contribute in certain areas of seal analysis and pre-testing. GEL will:

1. Perform a literature search on contact-type dynamic seals for alkali metal sealing application.
2. Perform an analytical investigation of screw seals for use with low viscosity fluids. Also conduct an experimental investigation of the helical groove seal using water as a working fluid. This investigation will be conducted under room ambient conditions.

3. Make calculations of the molecular flow from close gap seals exhausting to a vacuum. This calculation should include the effect of temperature and vapor pressure on leakage rates.

C. Progress Report

The 20,000 rpm water seal test rig was designed, manufactured, and setup prior to the beginning date of this program. Reference Figures 2, 3, 4, and 5. In this first reporting quarter, instrumentation and the test rig were checked out and first data was obtained. The data showed good agreement with previous calculations and no cavitation was experienced. Operation of the test rig was originally limited to 8000 rpm because of an insufficient air supply to the drive turbine. This problem was remedied by relocation of the rig near a 4 inch diameter air supply line. The turbine presently operates at 20,000 rpm with 20 horsepower loads. The occurrence of two bearing failures caused a delay in testing also. This problem has been eliminated by improvement in operating techniques and improved air-oil filtering.

Analytical investigation of screw seals has been started. The analysis is encouraging insofar as it indicates that turbulance - which will exist at the speeds considered - is likely to improve the pressure generating ability of the screw seal. Experimental results reported in the literature tend to confirm this prediction.

Water Pretesting of Rotating Fluid Ring Seals

There are presently three configurations of the stationary disk-rotating housing seal on hand at Evendale for testing in water, Figures 6a, 6b, and 6c. Testing on Configuration I was completed on July 13, 1962. The completion of testing on Configurations II and III is scheduled by July 31, 1962.

Design layouts have been completed on various configurations of the stationary housing-rotating disk and the squeeze seal. The layouts are presently being detailed to be available as hardware for testing in September.

Design work is in progress on the high speed test rig to be used for liquid metal testing and its auxiliaries required for liquid metal operation. Both should reach the procurement stage by the middle of September. These dates are indicated on the schedule, Figure 1.

II. BACKGROUND

A wide variety of seals have been used over many years for steam turbines, gas turbines, high pressure pumps, hydraulic equipment and, more recently, reactor coolant pumps. Many fluids, including liquid metals, have been effectively sealed for varying service periods. Considerable development effort has been spent in the seal area, yet, despite all accomplishments, we find seals to be a troublesome machine element and the cause of many failures and breakdowns.

Labyrinth and rubbing seals, used successfully in steam turbines, become questionable in aircraft gas turbines, due to thermal distortion and insufficient lubrication. Complete containment of fluids is usually accomplished by using expendable (or reclaimable) separating fluids. Hydrogen in large electric generators, for example, is sealed in by oil-flooded close-gap seals combined with labyrinth seals. Sealing of pump shafts in liquid metal cooled stationary nuclear reactors is usually accomplished by using inert gas as a separating fluid and then sub-dividing the seal into a liquid metal/inert gas and an inert gas/air seal. In one application, a freeze seal between sodium and inert gas and a rubbing seal backed up by an oil-filled labyrinth slinger seal between inert gas and air has been used. The first seal operates at the freezing temperature of sodium - 240°F - the second seal operates at 150°F. Shaft diameter is

5 inches; speed, 1180 rpm. Lubricated face seals for sealing between inert gas and air have also been used with limited success.

Mercury slinger seals for the sealing of a rotating shaft between the very low pressure in a mercury condenser and ambient air were introduced successfully by General Electric 25 years ago in mercury power plants. These seals are still in operation and turned out to be extremely trouble free and reliable. A similar seal was designed for a two-stage potassium test turbine which is being built and tested by the Flight Propulsion Laboratory. The potassium-to-argon seal portion consists of a potassium-filled slinger seal of the rotating channel type, and the argon to air seal is accomplished by a face seal. A labyrinth seal and forced circulation are used to prevent oil mist from contacting the potassium seal. "Zero" leakage in or out of the potassium system will be accomplished in this sealing arrangement.

"Zero leakage" when applied to seals in space, assumes a different meaning: it must include not only the working fluid, but also any buffer fluids used. Any fluid or gas used in the seals will be exposed to the vacuum of space, resulting in vaporization and the escape of gases and molecules, even through the smallest possible gap. Therefore, "zero leakage" can be closely approached, but not absolutely attained.

Hot metals and frozen liquids are prone to sublimation. Even diffusion of hot gases through metal walls will result in fluid losses. Molecular movements may be slowed down by using low temperatures and may also be influenced by ionization and magnetic fields. If, however, small leakages such as 0.1 lb. in 10,000 hrs. can be tolerated, then a number of sealing approaches can be identified as promising to accomplish this goal.

Because of zero gravity operating conditions, there is the problem of collecting and recirculating the liquid metal bearing and seal lubricants. Dynamic seals might serve the dual function of sealing and of pumping the lubricants back to the lubricant pump inlet. They could also provide the function of a lubricant pump.

Seal development should primarily concentrate on development of highly-reliable leakage-free dynamic vacuum seals. Availability of such seals would result in considerable progress in the art of turbo-electric space power systems. If the seal technology developed for vacuum seals can also be applied to the solution of in-loop-seal and recirculation problems, then a rigorous dynamic seal development program becomes even more desirable.

The basic rules in the development of vacuum seals in space power plants may be expressed as follows:

a. Sealing in space places a premium on temperature level and minimum cooling requirement due to the necessity of disposing heat by radiation, which becomes increasingly costly as temperatures are reduced.

b. Overall seal configurations in space power plants should be as short as possible to avoid creating a need for additional outside bearings. A turbogenerator arrangement, where the turbine is cradled between two bearings and the generator rotor overhung, is highly desirable if sealing can be accomplished between generator and turbine bearing.

c. Seals in space power plants should be self-contained and not depend on auxiliary systems. There is a premium on simplicity and on a minimum number of parts and materials involved.

d. Material choices must be restricted to those compatible with the working fluid. The fact that these materials will be free of surface oxides, due to the reducing action of the alkali metal and due to the absence of an oxidizing atmosphere should be fully considered.

The development of dynamic seals that will prevent leakage of the system working fluid over extended time periods (such as one year) into the vacuum of space can be accomplished in three steps:

1. Provide a pressure dam through which a transition from the high pressures of the working fluid in liquid or vapor state to the lowest pressure level possible may be accomplished.
2. Generate a clear separation between liquid and vapor phase of the working fluid and prevent direct leakage of liquid into the vacuum of space. Any leakage of liquid working fluid through even the most narrow gaps possible will be many times higher than leakage of working fluid in the vapor state through the same narrow gaps. Sealing will be most effective if a region of very low pressure vapor is established between the seal liquid and the final restriction through which the system is open to space.
3. Minimize the vapor pressure of the working fluid and the vapor leakage.

A pressure dam can be provided by a variety of concepts, resulting in high flow pressure drops or a counter pump action. Typical approaches are labyrinth, helical thread or slinger seals in various forms.

The novelty of the slinger and helical thread seals justifies their pre-testing with water as working the fluid. The information on the flow phenomena obtained in these preliminary tests can then be applied to the design of liquid metal seals. This application is possible through the use of dimensional similarity of the flow parameters; that is, viscosity, specific weight and Reynolds number. However, many phenomena, like heat transfer and erosion, cannot be simulated and studied in water tests, due to the different physical and chemical properties of the fluids.

III. ROTATING FLUID RING SEALS

A. Low Speed Test Rig Set Up

Preliminary seal experiments are presently being conducted using water as the working fluid. A 20,000 rpm seal test rig is presently being utilized to perform these experiments.

Operation of the water seal test rig with rotating housing-stationary disk Configuration I, (see Figure 2a) installed has been performed up to speed of 20,000 rpm and sealing pressures of 90 psi. Axial spacing of the stationary disc within the rotating housing has been maintained at $\frac{S_A}{a}$ = 0.167, 0.092 and 0.019 for test purposes. Partial evaluation of the dynamic seal testing has been completed and curves illustrating the data and discussion of the curves are enclosed.

The 20,000 rpm water seal test rig is installed in Building 301 at our Evendale, Ohio, facility. Test rig checkout was initiated on May 2, 1962. This checkout revealed the following problems which had to be resolved before scheduled testing could be accomplished.

1. Air Turbine Noise

The air turbine used to drive the rig was extremely noisy. Because of other operations in the same building it was necessary to reduce

this noise to an acceptable level. This was done by designing and installing an enclosure which muffled the air turbine.

2. Cooling Water Discharge

Cooling water is discharged overboard from the rotating housing. It was intended that this water would then collect in the annular water trap and drain overboard. Operation of the test rig proved that the water did not drain from the trap as planned. Instead, the water was discharged from the annular water trap in a heavy spray without passing through the drain. This problem was alleviated by repositioning the drain location to effectuate a positive drain.

3. Turbine Air Supply

Checkout of the test rig revealed that seal testing could not be accomplished at speeds higher than 8000 rpm because of air starvation at the turbine. The air supply line was inadequate to supply the power required to maintain seal operation at speeds higher than 8000 rpm. It was not feasible to install a high capacity air line to the test rig location. Therefore, it was necessary to move the rig to another location and install a short 2" air supply line. This change over was accomplished by June 13, 1962.

4. Instrumentation

Instrumentation problems were encountered in axial thrust and disk pressure measurement. One problem resulted in axial thrust measurement not being repeatable on the test rig. Subsequent investigation revealed that the bearings in thrust frame had brinelled the thrust transfer shaft. It was necessary to replace this shaft and reorient one of the bearings to improve the thrust measurement. The faulty disk pressure measurements were improved by employing better transducer mounting and calibration.

Checkout of the test rig in the new location with the improved air supply resulted in a spindle bearing failure at 13,000 rpm. The failure was caused by dirt in the bearing and on a bearing air seal. The failure was promptly resolved by bearing replacement and testing was resumed on July 11, 1962.

The water seal test rig is designed so that the following parameters are obtainable:

Housing speed

Frictional torque

Nitrogen pressure sealed

Water pressure on the stationary disk in eleven locations

Water flow for cooling

Axial thrust on the seal

Water in temperature

Water temperature at the circumference of the stationary disk

Balance air pressure

B. Water Test Data

1. Seal Capacity

Curves characterizing the slinger seal pressure capability are enclosed in Figures 7a, 7b, and 7c. The curves show the sealing pressure plotted versus the rotating housing angular velocity for various radius ratios. A calculated limit which corresponds to the case of having no water on the pressure side is indicated on each curve. However, this case of having no water on the pressure side is strictly an ideal situation and could never be reached in actual experiments. Therefore, the case of $\frac{a - r_N}{a} \rightarrow 0$ was the closest the calculated limit could be reached in actual experiments without blowing out the seal. In addition to determining the seal blow out point of each seal configuration, testing was done with various water immersions on the pressure side of the stationary disk. The experimental test points when plotted on sealing pressure versus rpm curves formed families of $\frac{a - r_N}{a}$ lines. A comparison of Figures 7a, 7b, and 7c indicate that the s/a ratio does not have a significant effect on sealing pressures with this configuration. It should be noted,

however, that the disk and rotating housing boundary layers were not submerged in any of the completed experiments.

Analysis of the plotted data revealed that the sealing pressure increase was proportional to the square of the rpm increase.

Prior to making plots of sealing pressure versus rpm plots were made of sealing pressure versus tip Reynolds number. Correlation between the separate test data points was improved, however, with the rpm plotted as the independent variable instead of Reynolds number. Review of the initial plots indicate that minor changes in viscosity did not have any significant effect on sealing capability.

2. Power Requirements

Curves characterizing the slinger seal power requirements are enclosed in Figures 8a, 8b and 8c. The curves show the slinger seal power requirement plotted versus the rotating housing angular velocity for various radius ratios.

A comparison of Figures 8a, 8b, and 8c indicates that the s/a ratio affected the power requirement. This effect was characterized by a decreasing power requirement as the stationary disk approaches the wall of the rotating housing. Analysis of the plotted data for this configuration revealed that the power requirement increase was approximately proportional

to the third power of the rpm increase. It could be seen from the data that greater disk immersions on the gap side required more power to drive the rotating housing. This was caused by an increase in ΔC_m, the frictional torque coefficient.

The cooling water flow which also acts as the working fluid affected the horsepower requirements. The effect was to increase the power requirements as the cooling flow increased. However, the power increase requirement was of an order of magnitude smaller than the frictional effect.

3. Frictional Torque Coefficient

Curves characterizing the slinger seal frictional torque coefficient are enclosed in Figures 9a, 9b, and 9c. The curves show the frictional torque coefficient plotted versus the Reynolds number at the disk tip for various radius ratios. The symbol ΔC_m was used in place of the standard C_m for frictional torque because the disk and housing were only partly immersed in the working fluid instead of completely immersed. The experimental test points when plotted on frictional torque coefficient versus disk tip Reynolds number curves form families of $\frac{a - r_N}{a}$ lines.

A comparison of Figures 9a, 9b, and 9c indicated that the s/a ratio affected the frictional torque coefficient. The effect was characterized

by a decrease in torque as the gap between the stationary disk and rotating housing on side A, (the water side) decreased. The line on each curve labeled $C_m = 0.0622\ R^{-1/5}$ represents an empirical equation derived by Dr. Hermann Schlichting for a fully submerged disk in the turbulent flow region. It should be noted that the experimental data from this test followed the same slope on the curve as Schlichting's equation. Analysis of the experimental data revealed that the frictional torque coefficient decrease is approximately proportional to the one-fifth power of the Reynolds number.

4. Seal Efficiency

Curves characterizing the slinger seal efficiency are enclosed in Figures 10a, 10b, and 10c. The sealing efficiency has been defined as the ratio of the maximum actual sealing pressure to the theoretical maximum sealing pressure. When considering the theoretical maximum sealing pressure the ratio of the water ring velocity to the housing velocity has been taken as unity. The enclosed figures show the seal efficiency plotted versus the dimensionless radius ratio, $\frac{a - r_N}{a}$.

A comparison of the enclosed figures indicated seal efficiency improved with increasing $S_{A/a}$, the disk-housing spacing.

5. Axial Force-Thrust

Curves characterizing the slinger seal axial force are enclosed in Figures 11a, 11b, and 11c. The figures show the hydrodynamic force plotted versus the slinger seal sealing pressure. This axial force or thrust was caused by the pressure unbalance on the stationary disk. An equal and opposite unbalance existed on the rotating housing.

A comparison of Figures 11a, 11b, and 11c indicate that increasing the gap between the stationary disk and rotating housing on side A, the water side, slightly increased the axial thrust.

6. Water Ring Velocity

Curves characterizing the slinger seal water ring velocity are enclosed in Figures 12a, 12b, and 12c. The curves show k, the ratio of the water ring angular velocity to the rotating housing angular velocity plotted versus the rotating housing angular velocity.

A comparison of Figures 12a, 12b and 12c revealed no significant effect on the water ring angular velocity when the axial spacing, S_A/a or the dimensionless radius ratios, $\frac{a - r_N}{a}$ was varied over a wide range. The experimental data indicates values of k range between 0.4 and 0.5.

C. Alkali-Metal Seal Test Facility

Preliminary diagrams of the dynamic seal alkali-metal test facility are shown in Figures 23 and 24. This arrangement has been tentatively selected based on previous alkali-metal test facility experience.

The system shown in the two figures has been designed to supply alkali-metal and argon. Flows up to 4 gpm of alkali-metal is supplied at any selected temperature from 300°F to 1400°F. The principle components, services and connections for measurement, purification and handling the alkali-metal are shown. Simplicity and reliability has been emphasized in the design of this loop.

IV. SCREW SEAL

A. Introduction

In recent years interest has increased in the helical screw pump for possible application as a dynamic shaft seal. When used as a sealing device, the screw pump is sometimes called a visco seal.

The screw pump has found wide application in the chemical industry for extruding viscous materials. It has also been used there as a very low specific speed pump. In the rotating machinery field, studies have been made to determine its suitability as a lubricating oil pump. In most all of these applications, however, the material being pumped was viscous and as such pump operation was observed only in the laminar range.

With the advent of the atomic energy and space programs where there is a need for a dynamic type seal for sealing gases and liquids of relatively low viscosity, interest has swung from the laminar operation of the visco seal to the turbulent operation. Although the principles of the operation of this type of device have been well explored and experimentally verified for the laminar flow case, no comparable theory exists for the turbulent case. In addition, no suitable criterion has been developed for determining the transition from laminar to turbulent screw pump operation.

B. Screw Seal Analysis

1. Laminar Flow Case

The screw pump consists of a threaded shaft rotating in a fixed cylinder or sleeve. The screw channel is constantly changing its position relative to sleeve and the advance of the fluid through the sleeve of the pump follows a helical path which is a mirror image of the helix on the screw. It has been shown, both analytically and experimentally, the end results would be the same if the screw were held stationary and the barrel rotated in direction opposite to the actual rotation of the screw, since the relative velocities of the screw and the barrel are unaltered. But in this case, the liquid moves along the helical path defined by the screw channel. Because the channel walls are attached to the screw, it is far easier to visualize and discuss the case in which the barrel rotates. For this reason, the screw is usually taken as the frame of reference.

Figure 13 shows a portion of a screw pump in which the rotational speed of the barrel is U. The component V tends to drag the fluid in the direction of the channel. The T component induces a transverse flow. This transverse flow is neglected in the analysis.

If part of the screw channel is isolated as shown in Figure 14, the flow in the screw pump can be considered as a special case of couette flow in an arbitrarily shaped channel against a pressure gradient. This

assumption is valid since in most applications the radius of the sleeve or rotor is usually much larger than the screw depth.

The differential equations governing this type of flow are the Navier Stokes equations. As shown in Reference 1, these equations, after removing the terms that vanish appear as

$$\frac{dp}{dx} = \mu \frac{\partial^2 U}{\partial y^2} \tag{1}$$

for incompressible laminar flow between two parallel plates.

A very simple solution of equation (1) is obtained for the case of steady flow between two parallel flat walls one of which is moving with a velocity V. The boundary conditions are:

$y = 0;\ U = 0$

$y = h;\ U = V$

The solution is

$$U = \frac{y}{h} V - \frac{h^2}{2\mu} \frac{dp}{dx} \frac{y}{h} \left(1 - \frac{y}{h}\right) \tag{2}$$

The flow through a channel of width b

$$Q = b \int_0^h U dy \tag{3}$$

$$Q = \frac{Vbh}{2} - \frac{bh^3}{12\mu} \frac{dp}{dx} \tag{4}$$

or

$$\frac{Q}{Vbh} = \frac{1}{2} - \frac{1}{12} \left[\frac{h^2}{\mu V} \frac{dp}{dx}\right] \tag{5}$$

In addition to the flow given by equation (4), there is a leakage through the clearance space δ. This is analyzed by assuming the flow is isothermal pressure flow through a narrow slot or

$$Q_L = \frac{\pi D \delta^3}{12 \mu b} \frac{dp}{dl} \tag{6}$$

where l is distance along the leakage path.

The factor E is a correction for possible eccentricity of the screw in the barrel. It varies from 1 for a perfectly centered screw to 2.5 for a screw with maximum eccentricity.

It is shown in Reference 2 that the leakage flow can be expressed as:

$$Q_L = \frac{\pi^2 D^2 \delta^3 \tan \phi}{10 \mu b L} \Delta P \tag{7}$$

or

$$\frac{Q_L}{Vbh} = \frac{\pi^2 D^2 \delta^3 \tan \phi}{10 h^3 \mu b^2 \sin \phi} \left(\frac{h^2}{\mu V} \frac{dp}{dx} \right) \tag{8}$$

or

$$\frac{Q_L}{Vbh} = \gamma \left(\frac{h^2}{\mu V} \frac{dp}{dx} \right) \tag{9}$$

where γ is a constant dependent only on the geometry of the screw.

The first term of equation (4) is the drag flow. The second term represents the backward flow along the channel due to the negative pressure

gradient. The total flow can be viewed as a drag flow minus a pressure flow and a leakage flow or:

$$Q = Q_d - Q_p - Q_L \tag{10}$$

By combining equations (5) and (9), the total flow in dimensionless terms becomes

$$\frac{Q}{Vbh} = \frac{1}{2} + \frac{1}{12} B + \gamma B \tag{11}$$

where $$B = -\frac{h^2}{\mu V} \frac{dp}{dx}$$

If $\frac{Q}{Vbh}$ is plotted versus B a straight line results with a negative slope as shown in Figure 15. Data for a given geometry of screw pump should all fall on one straight line independent of speed when plotted in the above dimensionless form.

For seal operation, the shut off pressure coefficient is of interest. For $Q = 0$, this becomes for the theoretical case,

$$\frac{h^2}{\mu V} \frac{dp}{dx} = \frac{1}{2\left(\gamma + \frac{1}{12}\right)} \tag{12}$$

The actual shut off pressure coefficient is lower than the theoretical. In practice, the sealing pressure is usually expressed as

$$\Delta P = K_1 \left(\frac{\mu V L}{h^2}\right) \tag{13}$$

The constant K_1, which depends on the geometry of the screw is determined experimentally, rather than from equation (12). The form of the equation has been verified experimentally, and values of the constant K_1 have been found for various screw geometries.

2. Transition Range

Frossel in Reference 4 presents data for various geometries of screw pumps over a speed range from 1500 to 15000 rpm. Typical pump characteristics are shown in Figures 16 and 17. In Figure 17 the data from 1500 to 12000 rpm fall on a straight line as the laminar theory would predict. The data for 13,500 rpm and 15,000 rpm, however, fall above the straight line characteristic. This is a Reynolds number effect caused by a decrease in the viscosity of the oil being pumped. The temperature of the oil increases as it passes through the pump lowering the viscosity and increasing the Reynolds number. At some critical value the flow becomes turbulent changing the pump characteristics.

To date no suitable criterion is available for predicting the transition point. The critical Reynolds number for an unloaded journal bearing may be a significant parameter;

$$Re_c = \frac{\rho V \delta}{u} \qquad (14)$$

Such a criterion works well for journal bearings, but the existence of threads on the screw pump may call for a different definition for the critical Reynolds number. It may be more accurate to base the Reynolds number on the screw geometry and obtain;

$$Re_c = \frac{\rho V d_n}{u} \tag{15}$$

where d_n is the hydraulic diameter of the screw passage. It will be one of the goals of the present study to determine a valid criterion for predicting the transition point.

3. Turbulent Flow Case

In Reference 5, a study is made of the hydrodynamic motion in a lubricant layer. The results of this study have direct application to the screw pump.

In order to describe turbulent flow in mathematical terms, it is convenient to separate it into a mean motion, $\bar{u}$, and a fluctuating motion u'.

The velocity and pressure components then become

$$u = \bar{u} + u' \qquad v = \bar{v} + v' \qquad w = \bar{w} + w' \qquad p = \bar{p} + p'$$

If the above are substituted in the Navier Stokes equations and a time average made, the following equations result for the physical situation of Figure 14b.

$$\frac{d\bar{p}}{dx} = \mu \frac{d^2 \bar{u}}{dy^2} + \frac{d}{dy} \left(-\rho \overline{u'v'}\right) \qquad (16)$$

$$\frac{d\bar{p}}{dy} = \frac{d}{dy} \left(-\rho \overline{v'^2}\right)$$

Upon comparison with equation (1), it is noticed that equations (16) contain an additional term, the so-called turbulent stress $\overline{u'v'}$. Further, there is a variation in pressure across the lubricant layer.

In order to integrate equation (16), it is necessary to know the turbulent stress $\overline{u'v'}$ beforehand. Constaninescu does this in Reference 5 by introducing Prandtl's mixing length, l, where

$$-\rho \overline{u'v'} = \rho l^2 \frac{d\bar{u}}{dy} \left| \frac{d\bar{u}}{dy} \right| \qquad (17)$$

After substituting equation (17) in equation (16) and simplifying he arrives at

$$A\bar{y}^2 \frac{d\bar{u}}{d\bar{y}} \left| \frac{d\bar{u}}{d\bar{y}} \right| + \frac{d\bar{u}}{d\bar{y}} + B\bar{y} - C = 0 \qquad (18)$$

where

$$A = K^2 Re \qquad B = -\frac{h^2}{\mu v} \frac{dp}{dx}$$

$$\bar{y} = y/h \qquad Re = \frac{\rho V h}{\mu}$$

Solution of equation (18) yields the velocity profile for various pressure coefficients and Reynolds numbers. It is instructive to compare the velocity profiles predicted by the laminar and turbulent theories. These are shown in Figure 18. The differences are very great. For the same pressure (B parameter) more flow will be delivered in turbulent flow than in laminar. This is also borne out by the data of Frossel in Figures 16 and 17.

If the couette flow velocity profile is plotted for various Reynolds numbers, Figure 19 results. The Reynolds number has substantial influence upon the velocity profile; when $Re \longrightarrow 0$ the velocity profile tends towards the laminar one and when $Re \longrightarrow \infty$ the velocity distribution tends to become constant with respect to y. It is more important to note that the area under the velocity distribution curve is independent of Reynolds number. This means that the drag flow term, $Q_L = \frac{Vhb}{2}$, in equation (4) is also independent of Reynolds number.

Now if velocity is plotted for a constant value of pressure coefficient $B = -20$, the influence of Reynolds number is clearly seen. This is shown in Figure 18.

The mean velocity in the screw channel can be thought of as consisting of two parts.

$$u_m = u_{m_c} + u_{m_p} \tag{19}$$

where u_{m_c} = mean couette velocity

u_{m_p} = mean pressure velocity

Figure 19 shows that u_{m_c} is independent of Reynolds number. The mean velocity is then

$$u_m = 5v + u_{m_p} \tag{20}$$

For laminar flow, neglecting seal leakage, this becomes

$$\frac{u_m}{V} = \frac{1}{2} + \frac{B}{12} \tag{5}$$

For turbulent flow, u_{m_p} is a function of Reynolds number. Mean velocity for various Reynolds numbers and various B parameters were calculated in Reference 5. This is shown in Figure 21 for the pertinent range of values. The pressure coefficient is almost linear for all Reynolds numbers. This can be expressed analytically as

$$B = K\left(\frac{u_{m_p}}{V}\right)^n \tag{21}$$

where $K = 12$ for $Re = 0$ and $K = \infty$ for $Re \longrightarrow \infty$.

This variation can be expressed as

$$K = K_o + K_1 \, Re^n$$

$$= 12 + 0.14 \, Re^{0.725} \tag{22}$$

Substituting for u_{m_p} in equation (20), we obtain

$$\frac{Q}{Vbh} = \frac{u_m}{V} = \frac{1}{2} + \frac{B}{(K_o + K_1 \, Re^{0.725})} \qquad (23)$$

$$\frac{Q}{Vbh} = \frac{u_m}{V} = \frac{1}{2} + \frac{B}{(12 + 0.14 \, Re^{0.725})} \qquad (24)$$

For Reynolds number = 0, this reduces to the laminar case. The dimensionless pressure coefficient versus the dimensionless flow coefficient is plotted in Figure 22.

It is interesting to compare the theoretical screw pump characteristics with typical measured characteristic of Frossel in Figure 16 and 17. If the flow in the pump were laminar and isothermal all of the data points would lie on one straight line when the dimensionless pressure coefficient was plotted against dimensionless flow coefficient. This held true at low rotational speeds, but at higher speeds a fan shaped family of characteristics was obtained. Since the pumps tested by Frossel were not cooled, the temperature of the oil increased as it passed through the pump with an attendant decrease in viscosity and increase in Reynolds Number. The effect is a minimum at high flows since the temperature rise is smaller due to the higher mass rate. At low flows and high speeds the temperature rise if greater giving a larger negative slope to the characteristic. For this reason, along any speed line the slope of the characteristic becomes steeper as the pump operating point moves to lower flows. The dip on the characteristic lines at high rotational speeds is most likely a result of the flow

changing from laminar to turbulent conditions. The above theoretical analysis predicts the same shape of characteristic as was experimentally observed by Frossel.

When the screw pump is adapted for use as a seal, the important point on the characteristic is the shut off pressure, i.e. the value of pressure coefficient at zero flow.

From equation (24), the shut off value is given by

$$\frac{dp}{dx}\frac{h^2}{\mu v} = \frac{1}{2}\left(12 + 0.14\ Re^{0.725}\right) \qquad (25)$$

The constants in the above equation are the theoretical values. It was shown for the laminar case that the experimentally determined constant was considerably lower than the theoretical maximum. A similar discrepancy between the theoretical and actual would be expected in the turbulent case. Thus we would expect an expression for the turbulent sealing pressure to be of the form

$$\Delta P = \left(K_1 + K_2\ Re^m\right)\left(\frac{\mu U L}{h^2}\right) \qquad (26)$$

where the constants in the equation will be function of the screw geometry. The verification of the form of equation and the determination of the constants K_1 and K_2 will comprise an important part of the screw seal study.

Since Frossel (Reference 4) did not actually measure shutoff pressure, it is not known for certain that entrapolating his measured pump characteristics to zero flow is valid. Oil foaming or cavitation may take place causing the seal effect to breakdown at high Reynolds number. Based on the analytical study presented above, however, it appears that the seal operation should improve with increasing Reynolds number.

SYMBOLS

1. Slinger Seal

R	Reynolds number, taken at the disk tip, dimensionless, $\frac{wa^2}{\nu}$.
C_m	Torque coefficient for disk partially wetted on two sides, dimensionless, $\frac{2M}{\rho \omega^2 a^5}$
P_N	Static pressure of the nitrogen being sealed by the water, psig.
$P_{Dynamic\ A}$	Dynamic pressure of sealing fluid, water, on the atmospheric side of the disk, psig.
a	Radius of stationary disk, ft.
r_A	Radius of fluid from the center of the disk on the atmospheric side, ft.
r_N	Radius of fluid from the center of the disk on the nitrogen side, ft.
ν	Kinematic viscosity, ft^2 per second.
ρ	Sealing fluid mass density, lb sec^2/ft^4.
k	Ratio of angular velocities, dimensionless, $\frac{\beta}{\omega}$
ω	Angular velocity of rotating housing, radians per second.
N	Rotating housing velocity, rpm
β	Angular velocity of sealing fluid, water, radians per second.
M	Frictional torque (moment), ft. lb.
$\frac{a - r}{a}$	Radius Ratio, dimensionless
W	Cooling flow, gpm water

s_A	Spacing between disk and rotating housing on the atmoshperic side of the disk, ft.
η	Seal efficiency
F_N	Thrust
HP	Horsepower

2. Screw Seal

A	Constant in turbulent flow equation (18)
b	Width of thread channel
B	Dimensionless pressure
C	Constant in turbulent flow equation
d_h	Hydraulic diameter of screw channel
D	Shaft diameter
e	Flight width
E	Eccentricity correlation factor
h	Depth of groove in shaft
k	Constant turbulent pressure sealing equation (21)
k_1	Constant in turbulent pressure sealing equation (22)
k_2	Constant in turbulent pressure sealing equation (22)
k_1	Constant in laminar and turbulent pressure sealing equations (13) and (26)
K_2	Constant in turbulent pressure sealing equation (26)
l	Distance along shaft

L	Threaded shaft length
m	Constant turbulent pressure sealing equation (26)
n	Constant in relation between pressure coefficient and mean pressure velocity (21)
N	Shaft angular velocity
P	Pressure
ΔP	Pressure drop across seal
Q	Volume flow
Re	Reynolds number
t	Thread pitch
u	Velocity in x direction
v	Shaft velocity
v	Velocity in y direction
V	Velocity of moving plate
w	Velocity in z direction
x	Distance along axes of thread groove
y	Distance along direction of groove depth
z	Distance along direction of groove width
γ	Constant depending on groove geometry
δ	Radial clearance between shaft and sleeve
μ	Absolute viscosity
ρ	Fluid density

Subscripts

m	mean value
c	couette flow value
p	pressure flow value

Superscripts

'	fluctuating value
—	time averaged value

REFERENCES

1. Schlichting, H.: Boundary Layer Theory, Pergamon Press, New York, 1955.

2. Carley, J. F. and Strub, R. A.: Industrial and Engineering Chemistry, Vol. 45, No. 5, May 1953.

3. Stair, W. K.: "The Visco Seal - A Survey," University of Tennessee Engineering Experiment Report No. ME-5-62-2, March 1962

4. Frossel, W.: "Hochtourige Schmierolpumpe," Konstruktion, Vol. 12, No. 5, 1960, pp. 195-203.

5. Constantinescu, V. N.: "On Turbulent Lubrication," Proc. Instn. Mech. Engr., Vol. 173, No. 38, 1959.

6. Dushmen, "Vacuum Technique," John Wiley, 1959.

Start △

Complete ○

Figure 1. Dynamic Seal Work Schedule

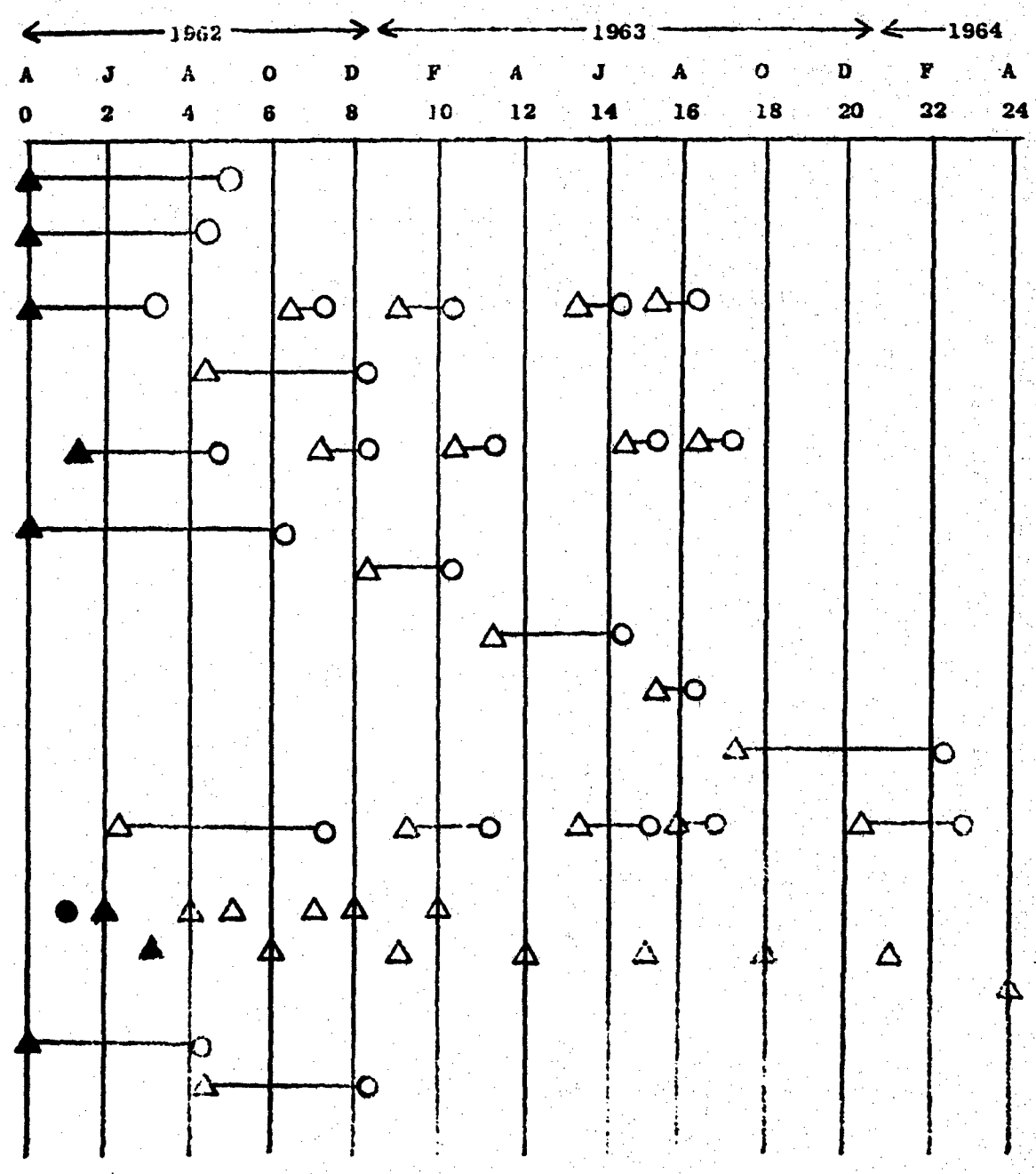

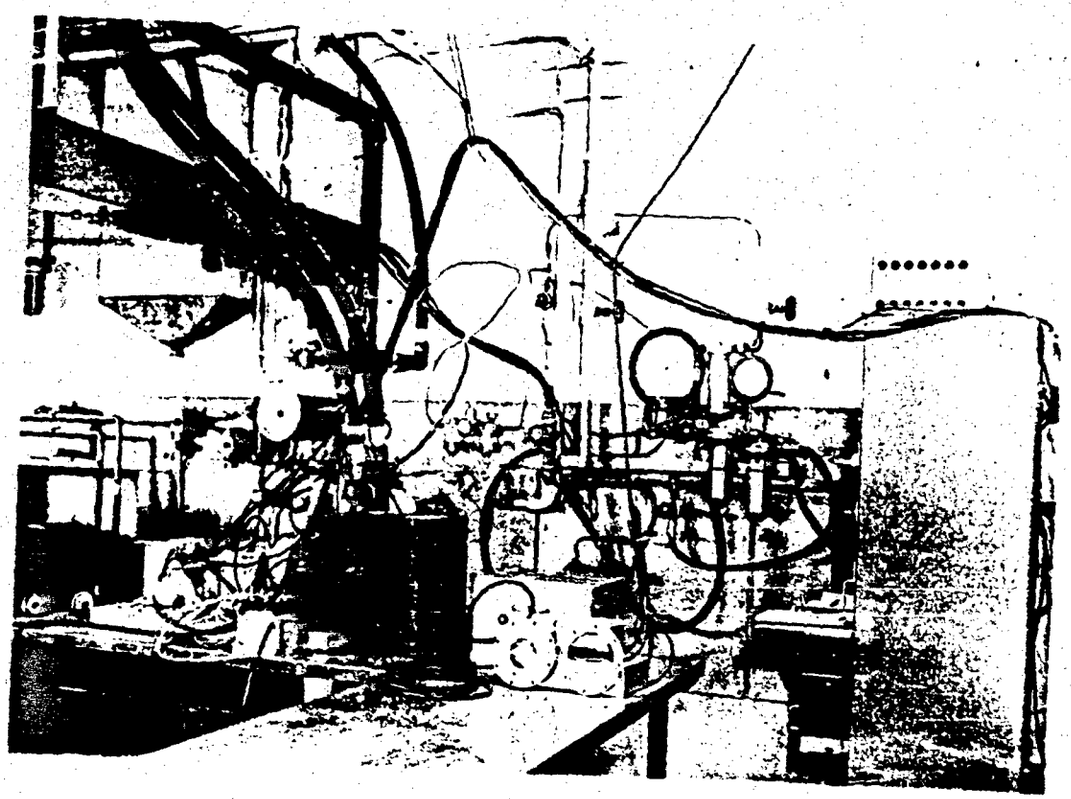

Figure 2. Seal Test Rig

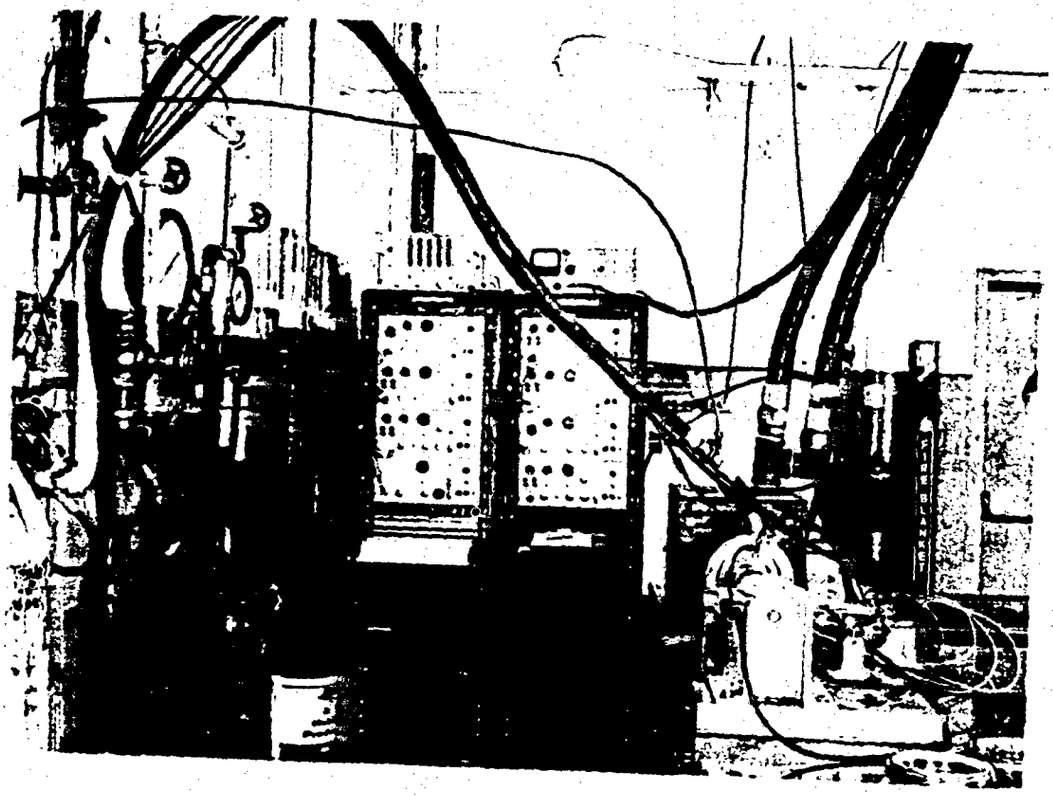

Figure 3. Seal Test Rig

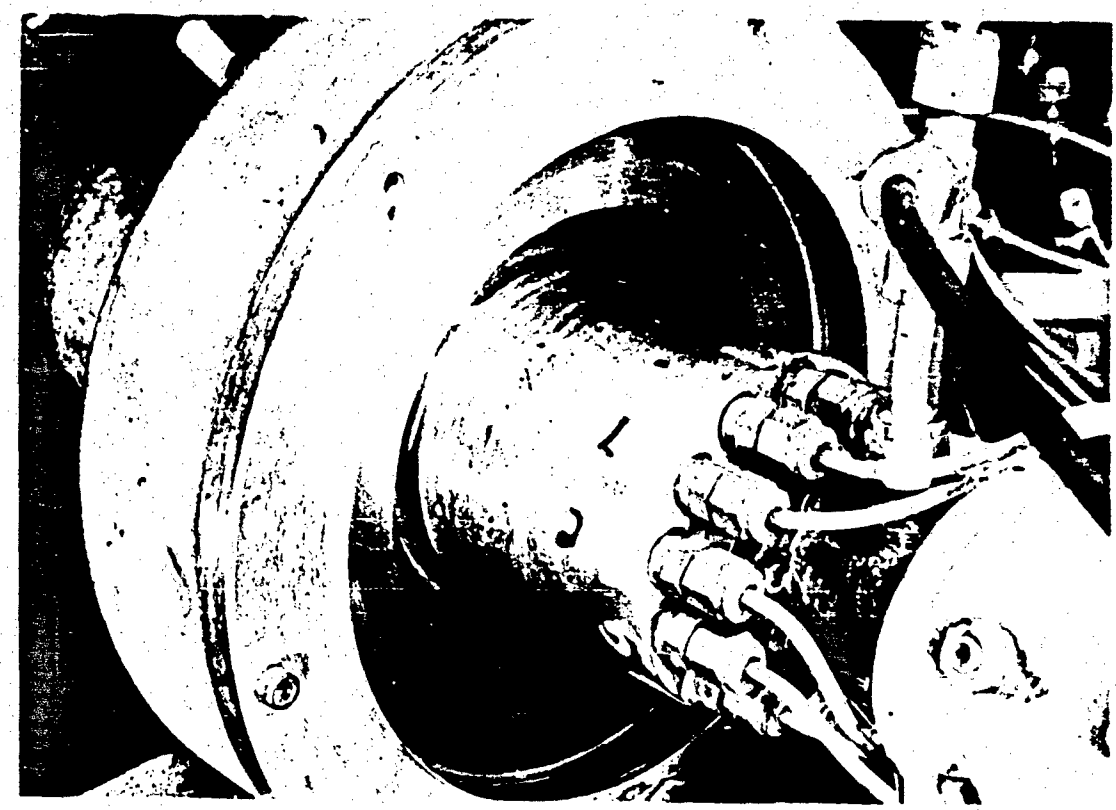

Figure 4. Seal Test Rig

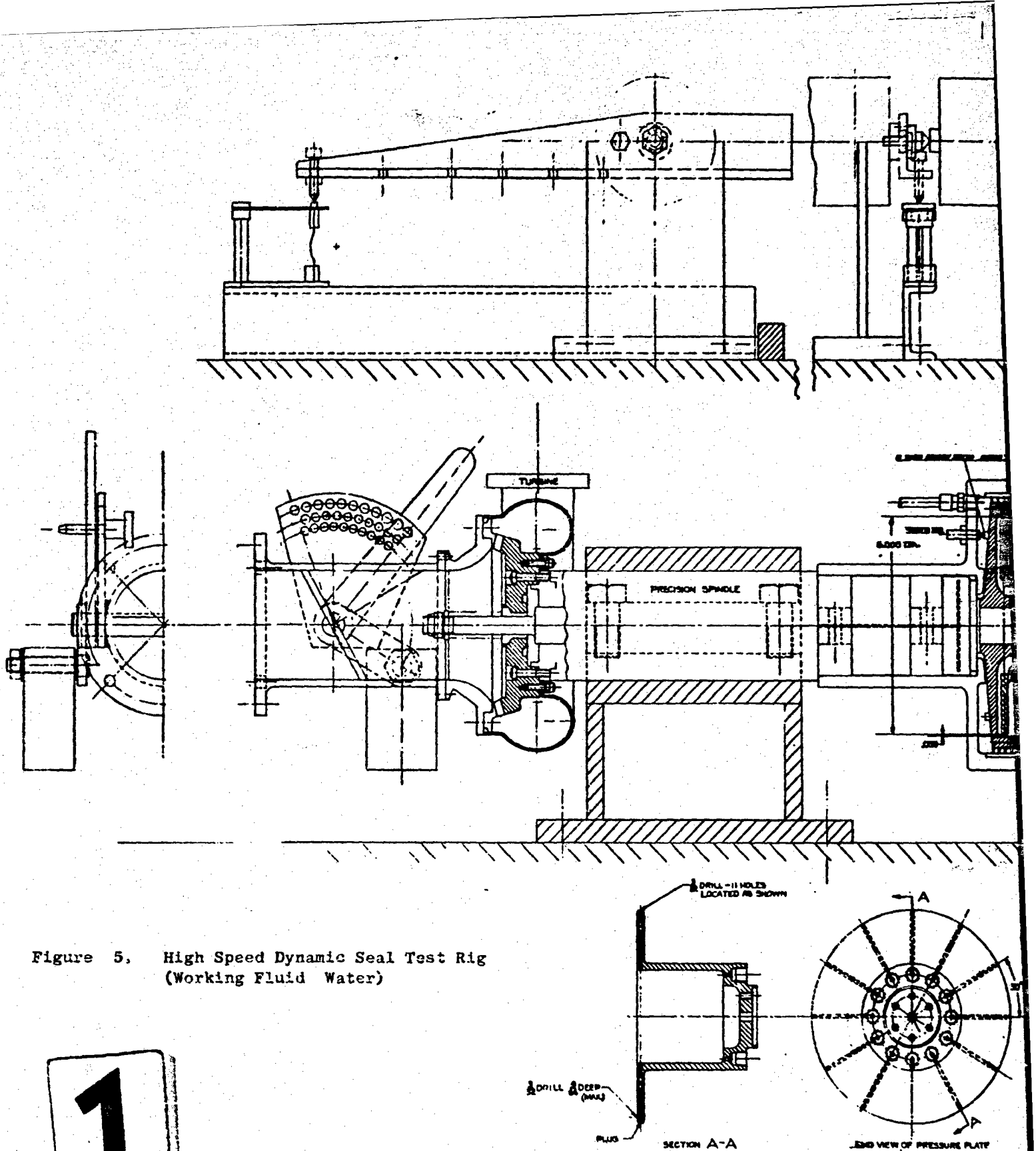

Figure 5. High Speed Dynamic Seal Test Rig (Working Fluid Water)

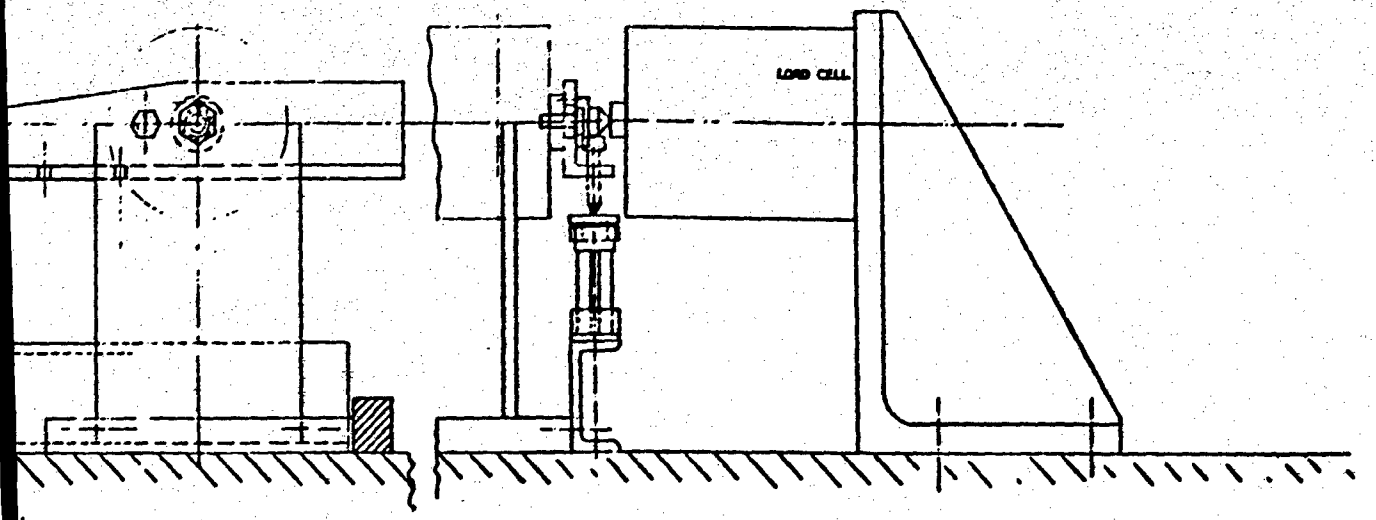
LOAD CELL

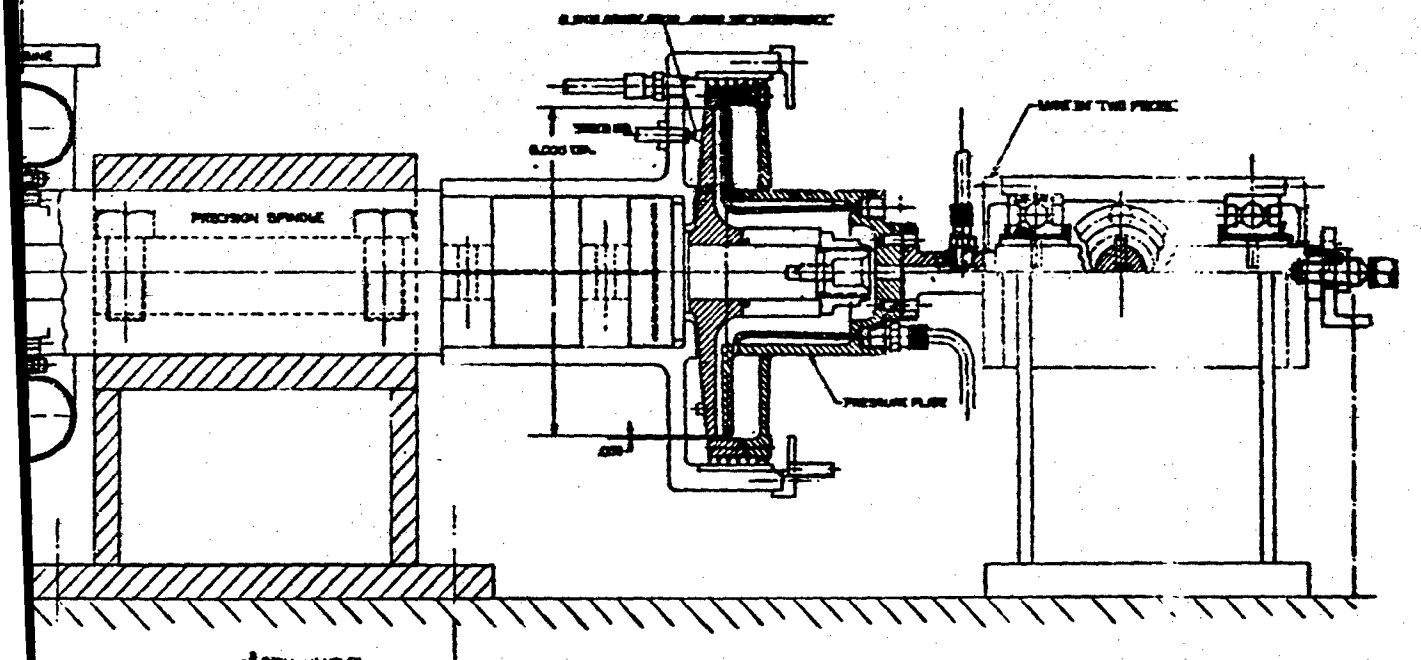
PRECISION SPINDLE
PRESSURE PLATE

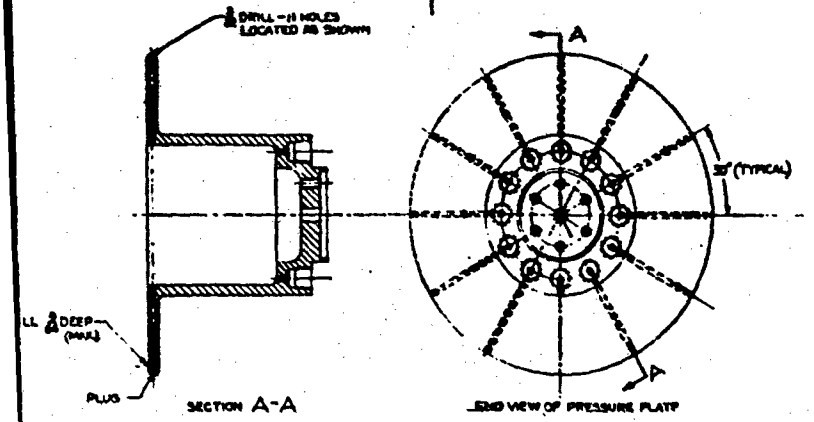
DRILL -11 HOLES LOCATED AS SHOWN
DEEP (MIN.)
PLUG
SECTION A-A
A
A
30° (TYPICAL)
END VIEW OF PRESSURE PLATE

2

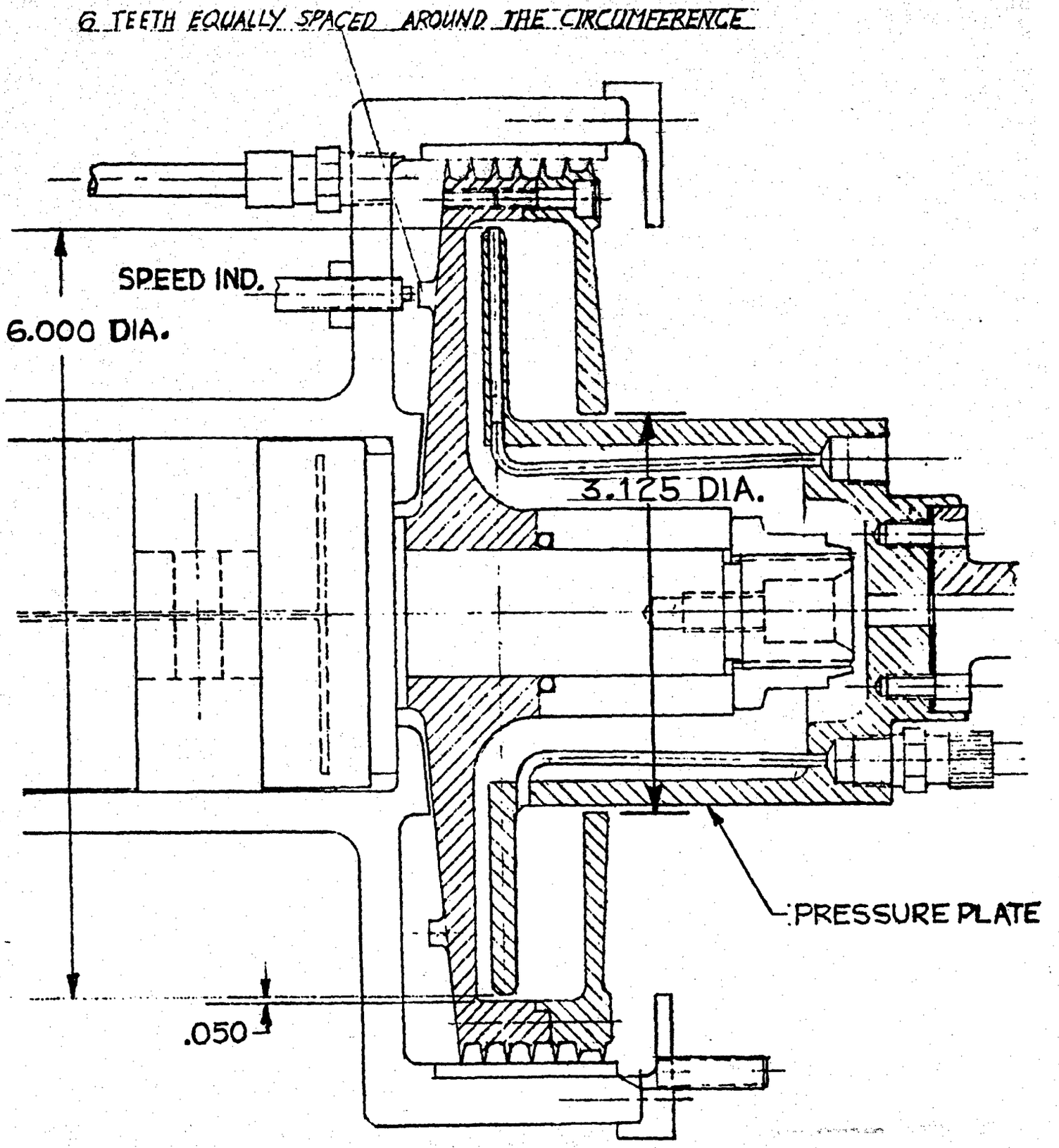

Figure 6a. Housing-Disk Configuration I, Actual Size, $\frac{rA}{s} = 0.52$.

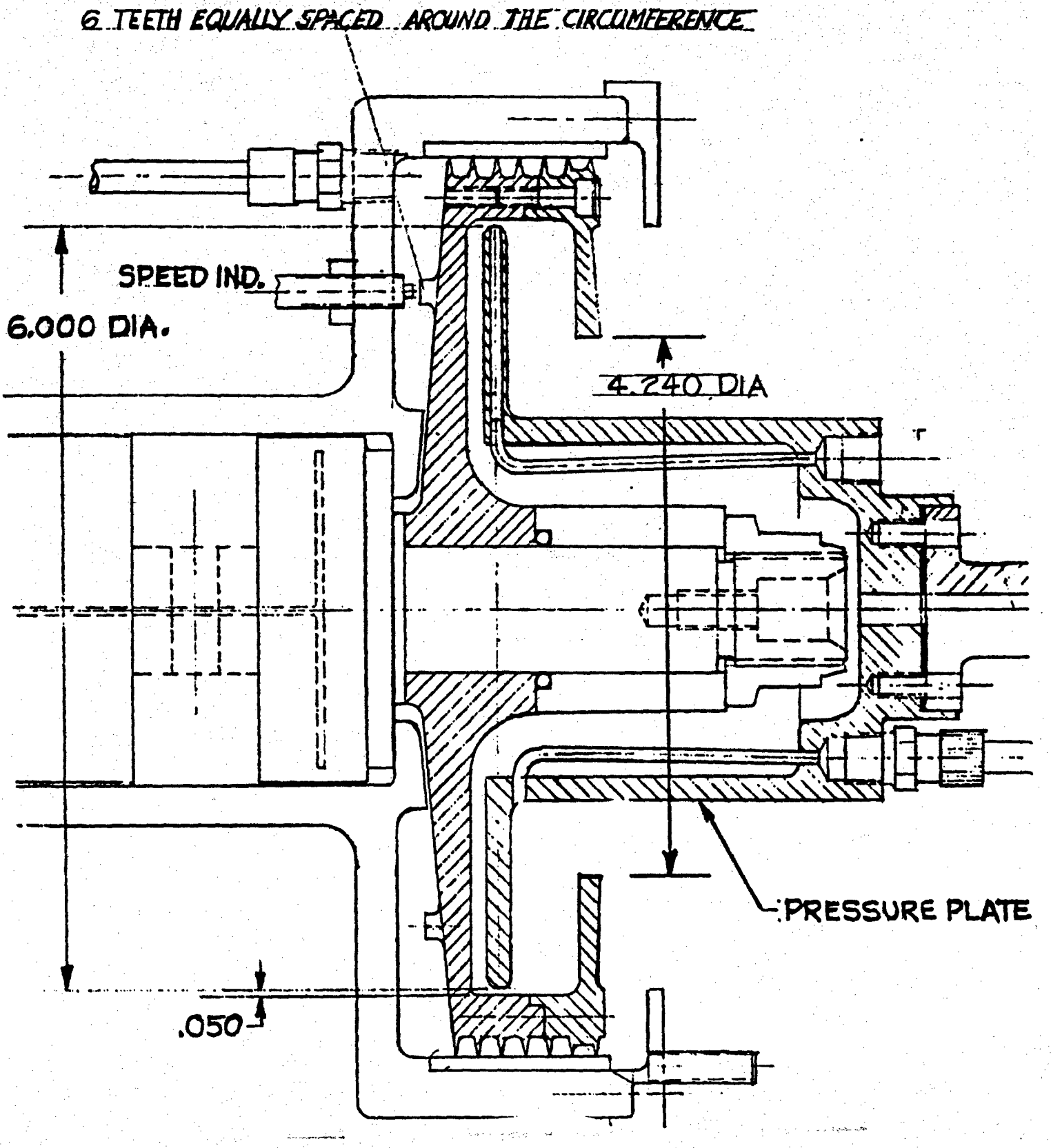

Figure 6b. Housing-Disk Configuration II, Actual Size, $\frac{r_A}{a}$ - 0.71.

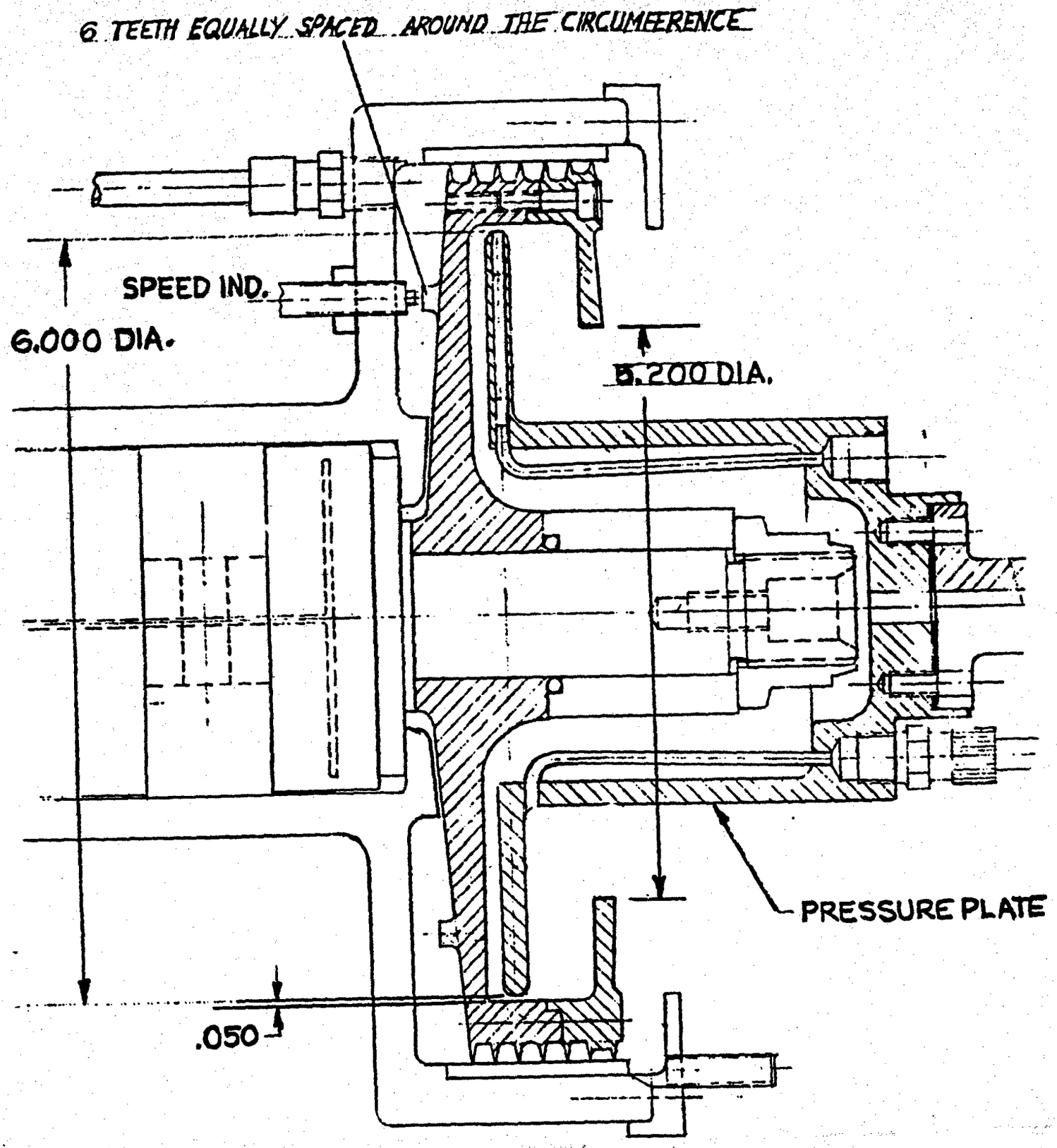

Figure 6c. Housing-Disk Configuration III, Actual, $\frac{rA}{a} = 0.87$.

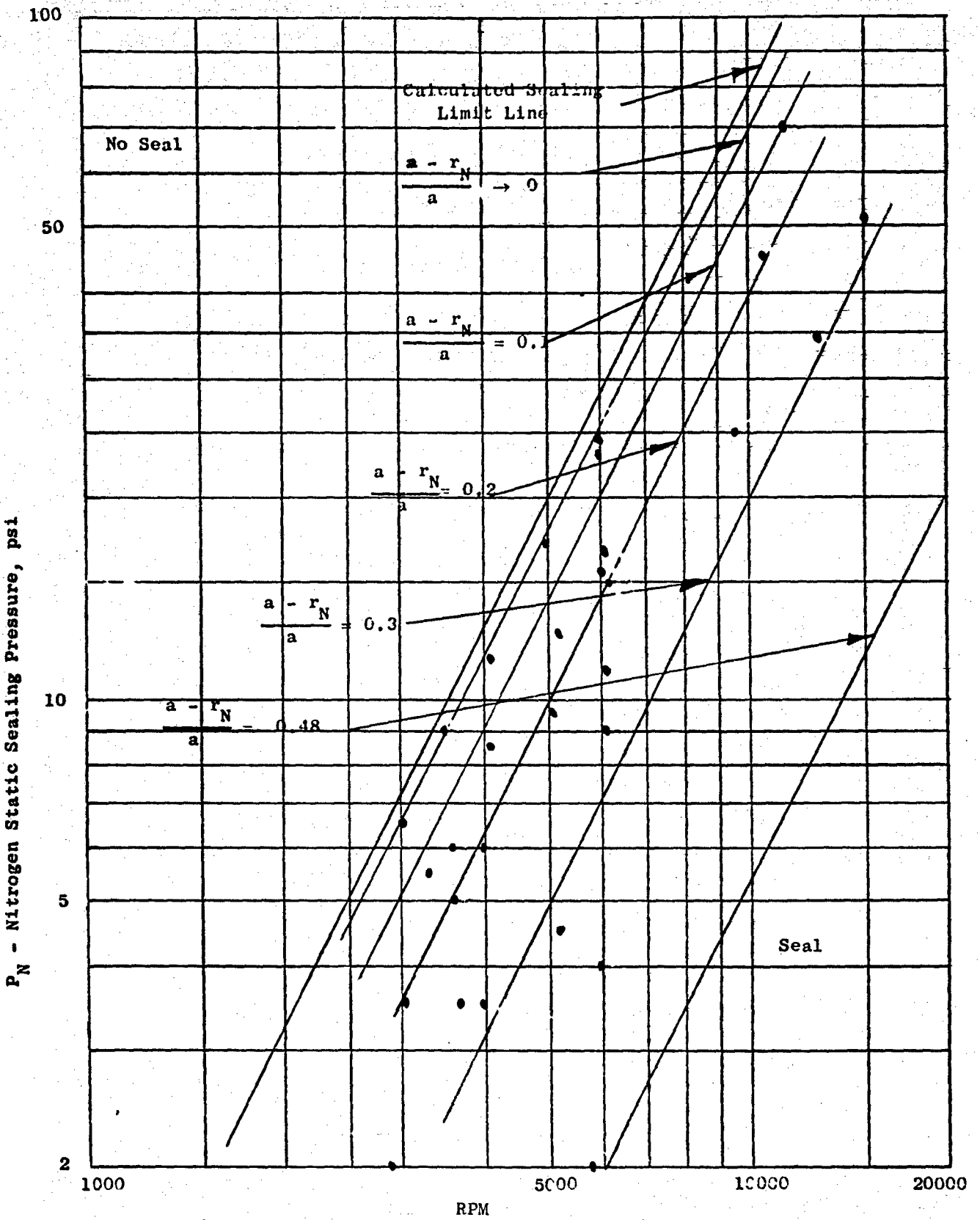

Figure 7a. Slinger Seal Pressure Capacity, $\frac{rA}{a} = 0.52$, $\frac{SA}{a} = 0.167$.

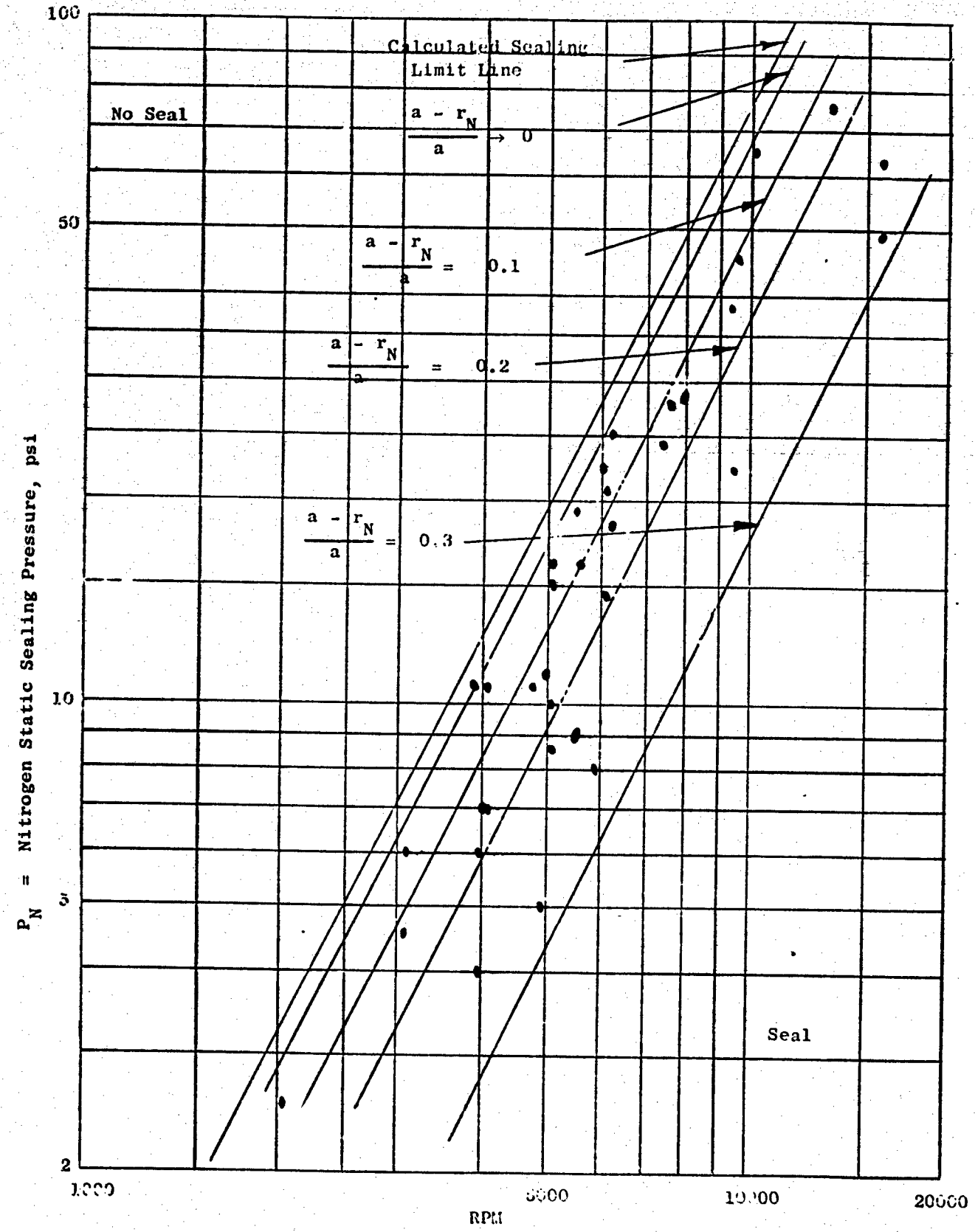

Figure 7b. Slinger Seal Pressure Capacity, $\frac{rA}{a} = 0.52$, $\frac{SA}{a} = 0.092$.

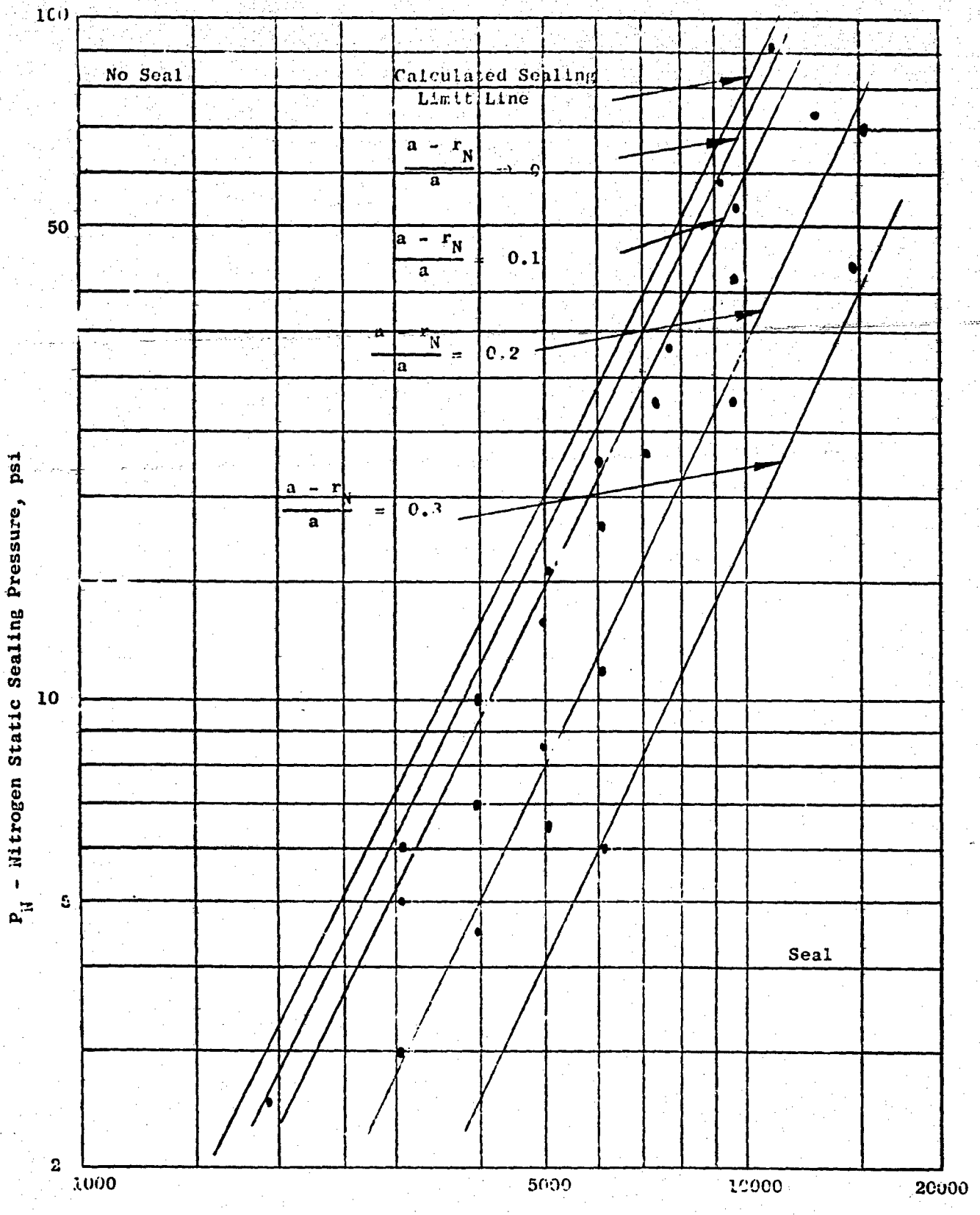

Figure 7c. Slinger Seal Pressure Capacity, $\frac{rA}{a} = 0.52$, $\frac{SA}{a} = 0.019$.

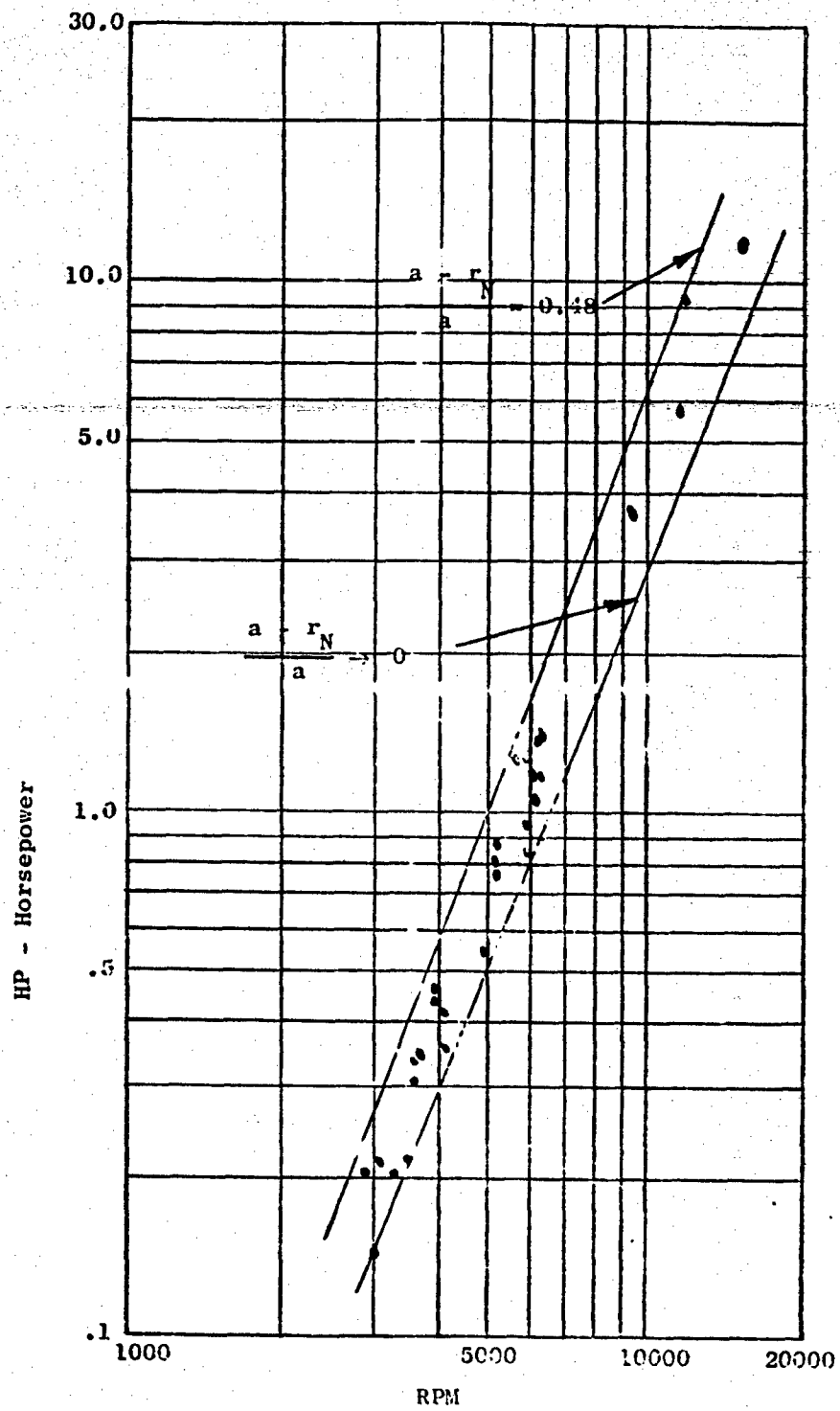

Figure 8a. Slinger Seal Power Requirement, $\frac{rA}{a} = 0.52$, $\frac{SA}{a} = 0.167$.

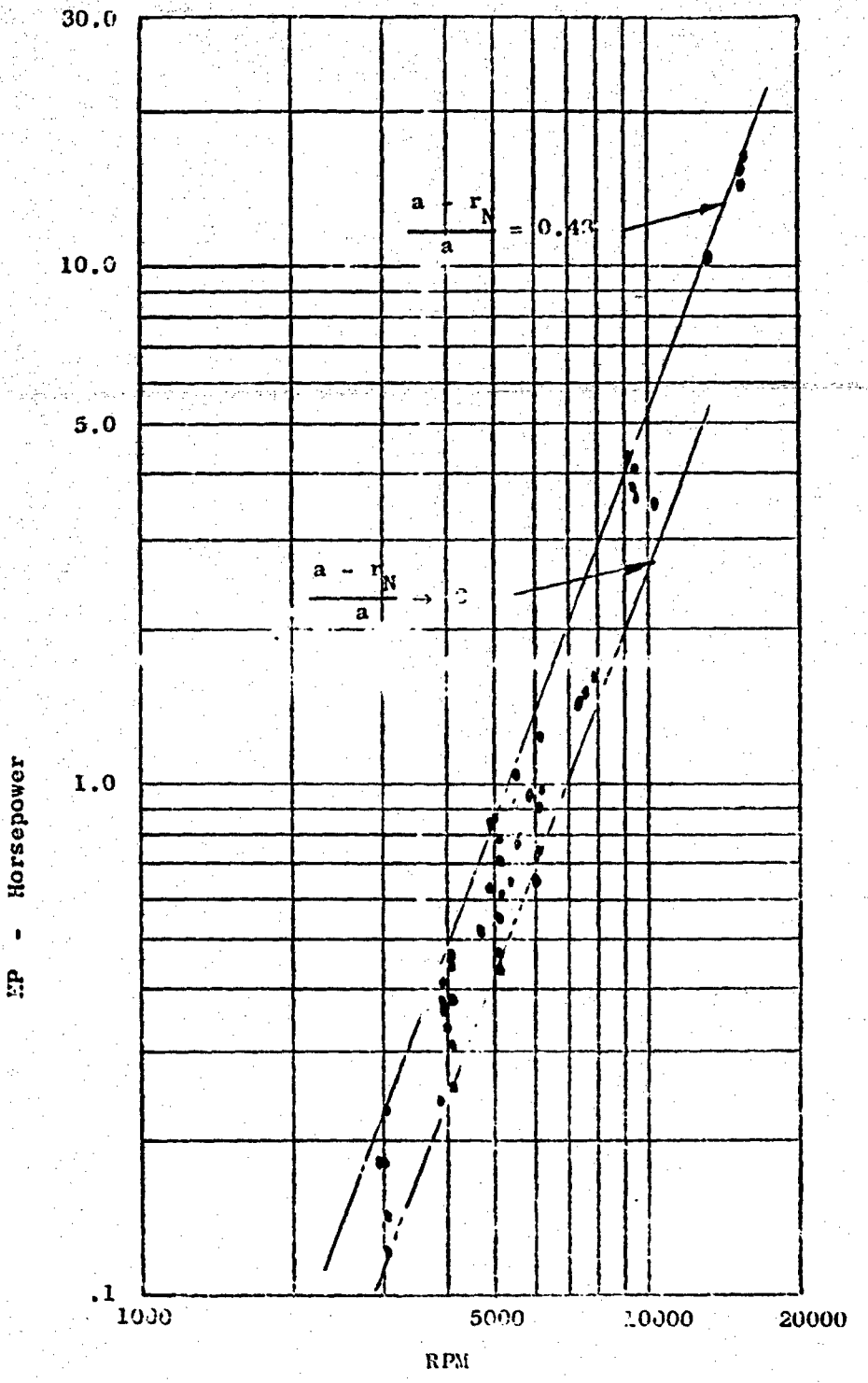

Figure 8b. Slinger Seal Power Requirement, $\frac{rA}{a} = 0.52$, $\frac{SA}{a} = 0.092$.

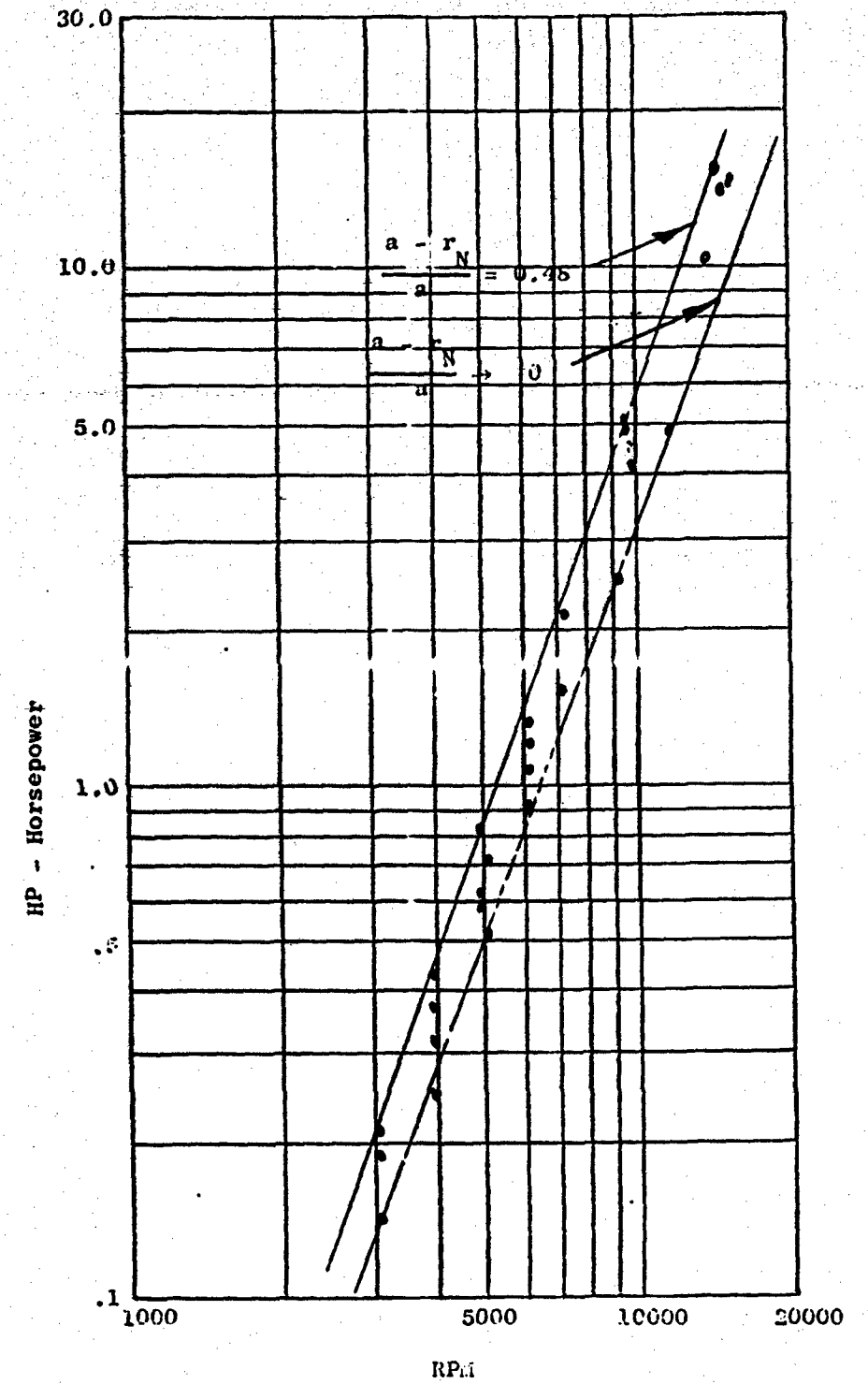

Figure 8c. Slinger Seal Power Requirement, $\frac{rA}{a} = 0.52$, $\frac{SA}{a} = 0.015$.

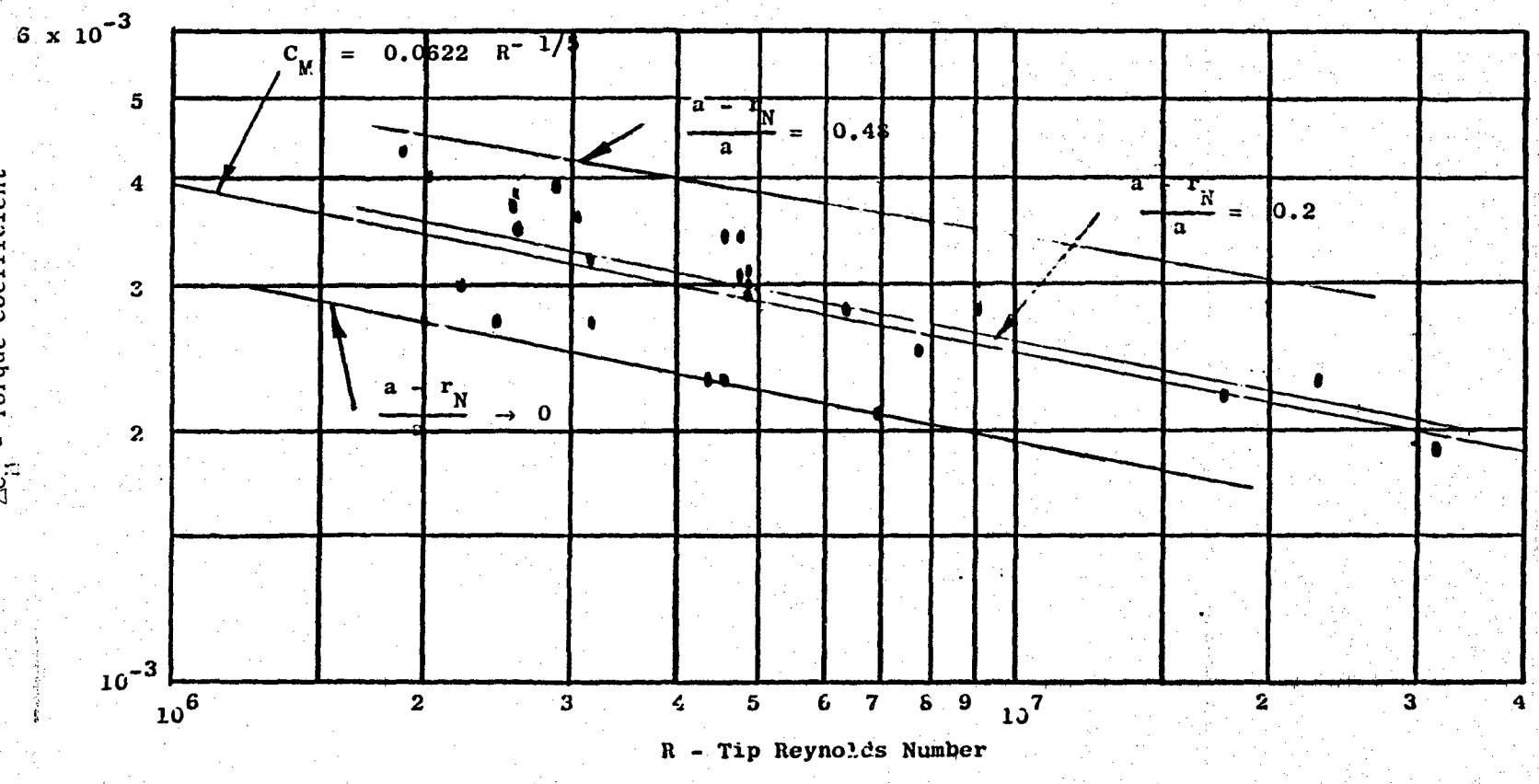

Figure 9a. Slinger Seal Torque Coefficient, $\frac{rA}{a} = 0.52$, $\frac{SA}{a} = 0.167$.

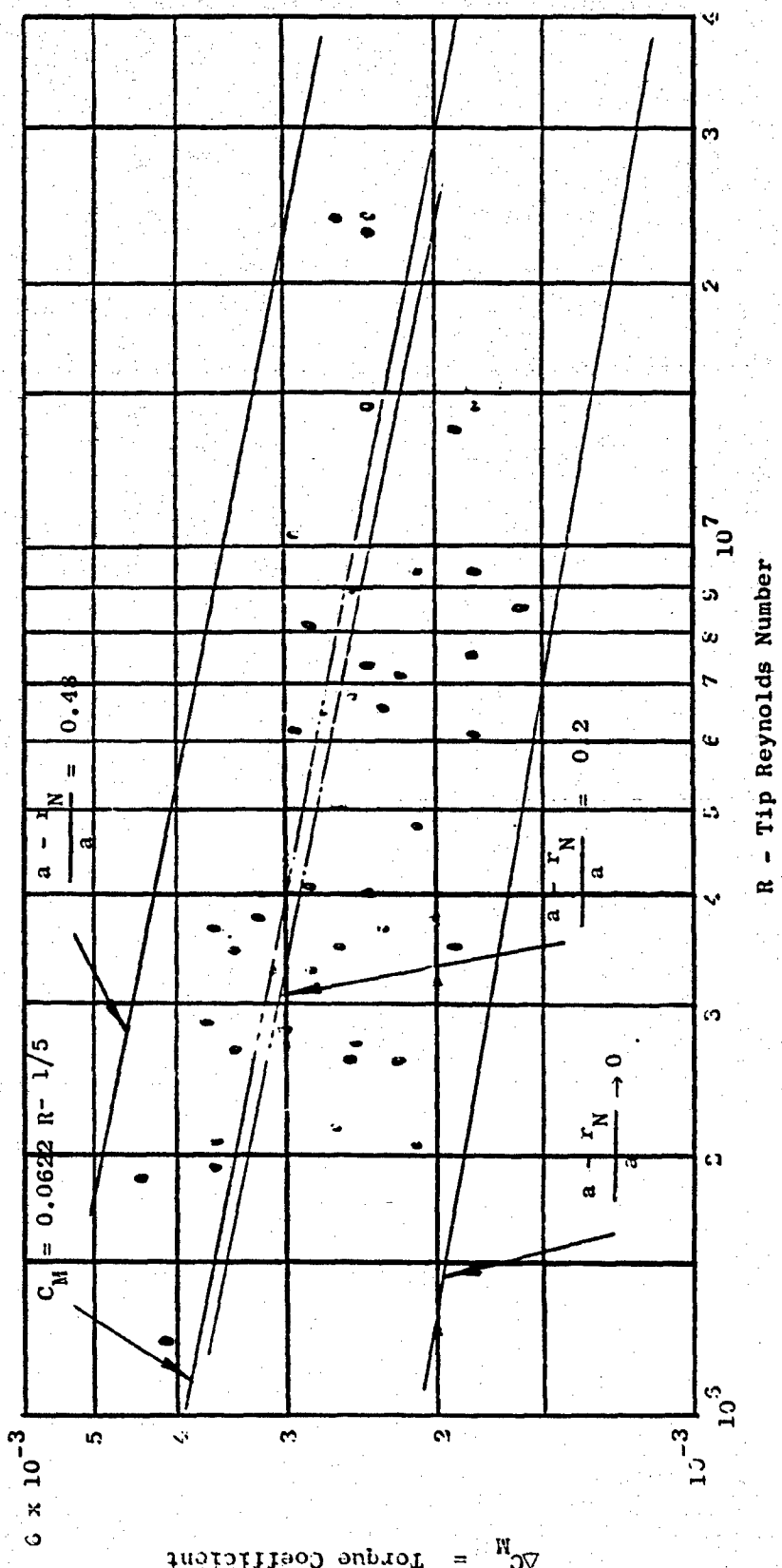

Figure 9b. Slinger Seal Torque Coefficient, $\frac{rA}{a} = 0.52$, $\frac{SA}{a} = 0.092$.

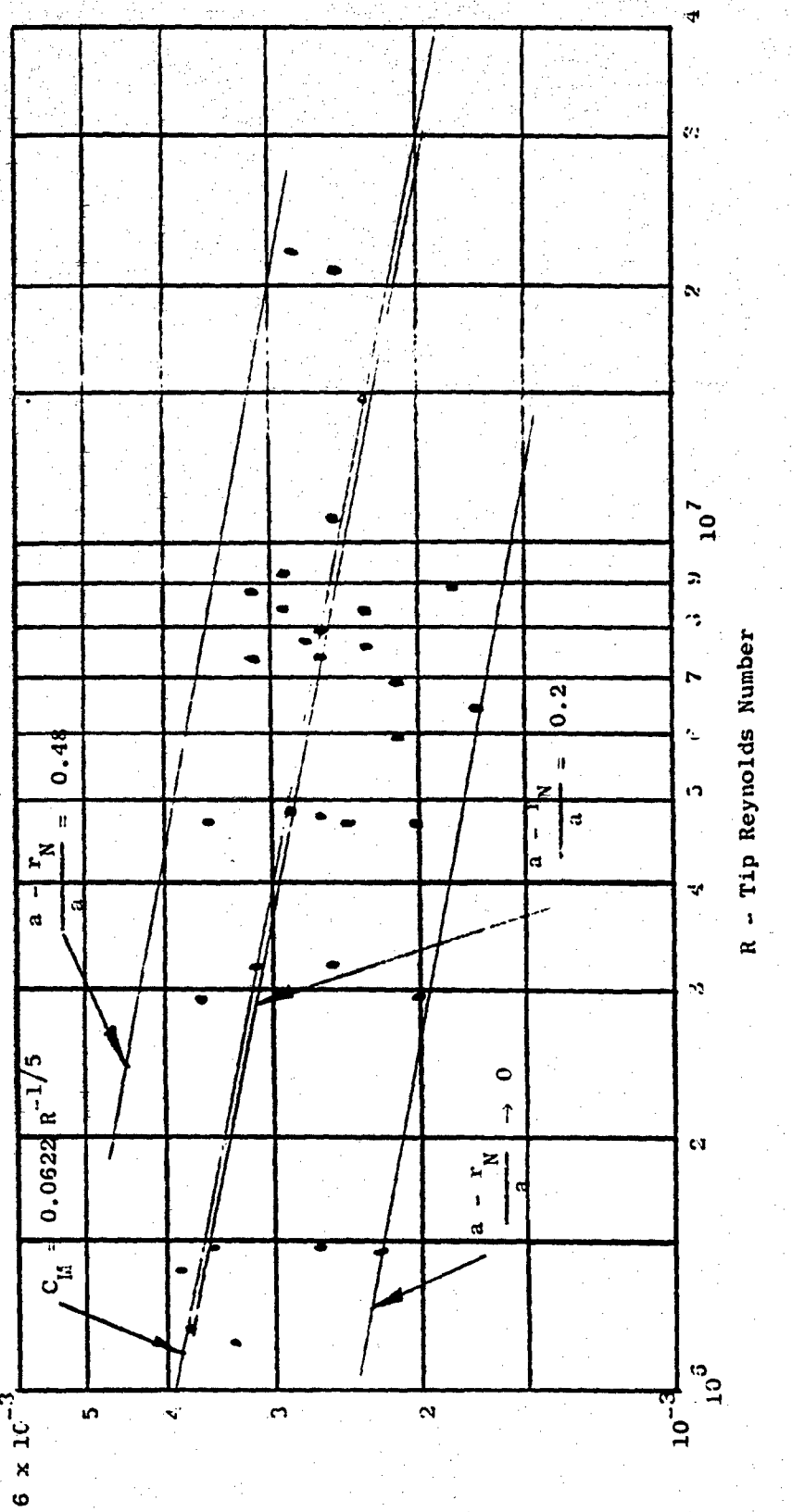

Figure 9c. Slinger Seal Torque Coefficient, $\frac{rA}{a} = 0.52$, $\frac{SA}{a} = 0.019$.

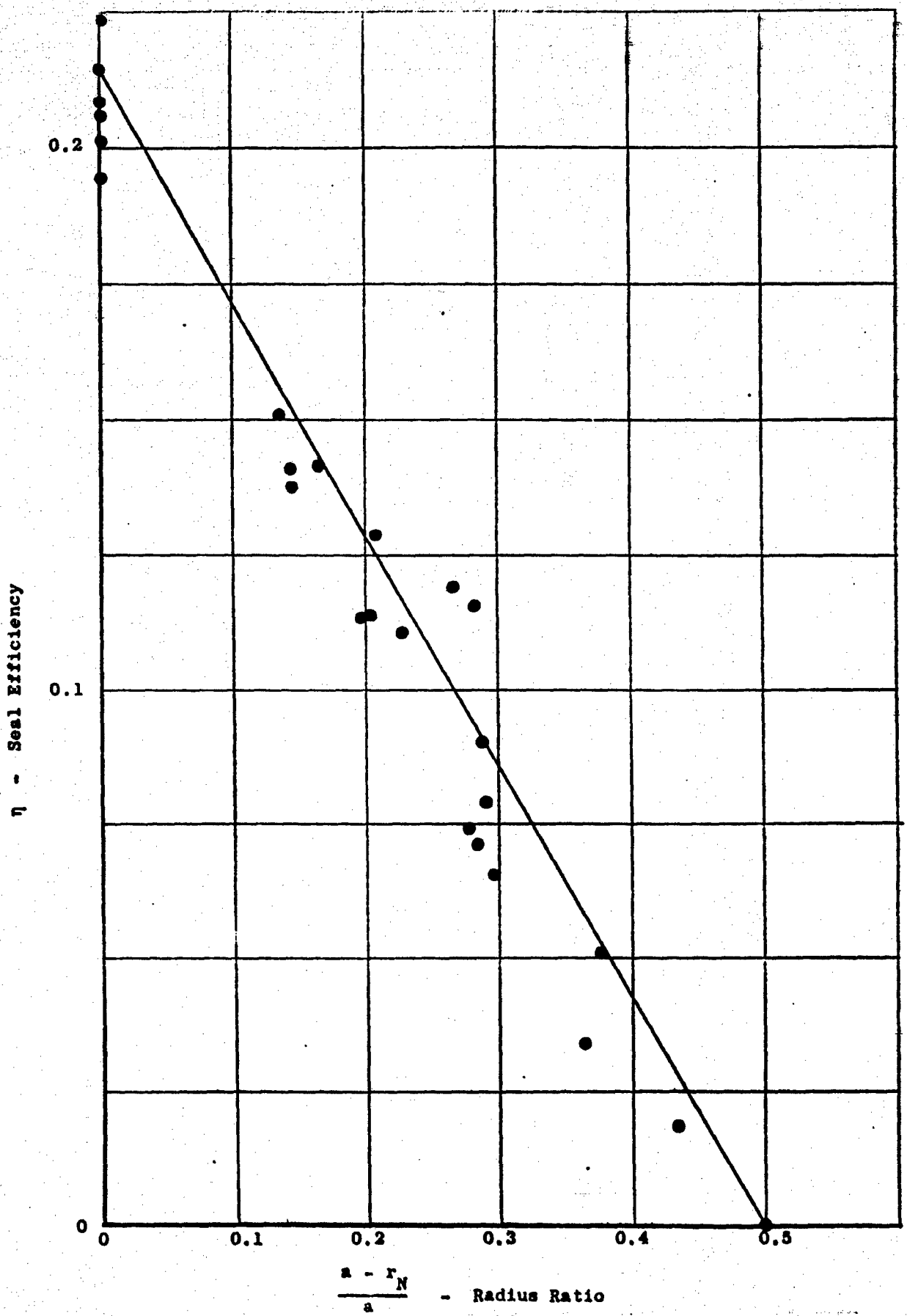

Figure 10a. Slinger Seal Efficiency $\frac{rA}{a} = 0.52$, $\frac{SA}{a} = 0.167$.

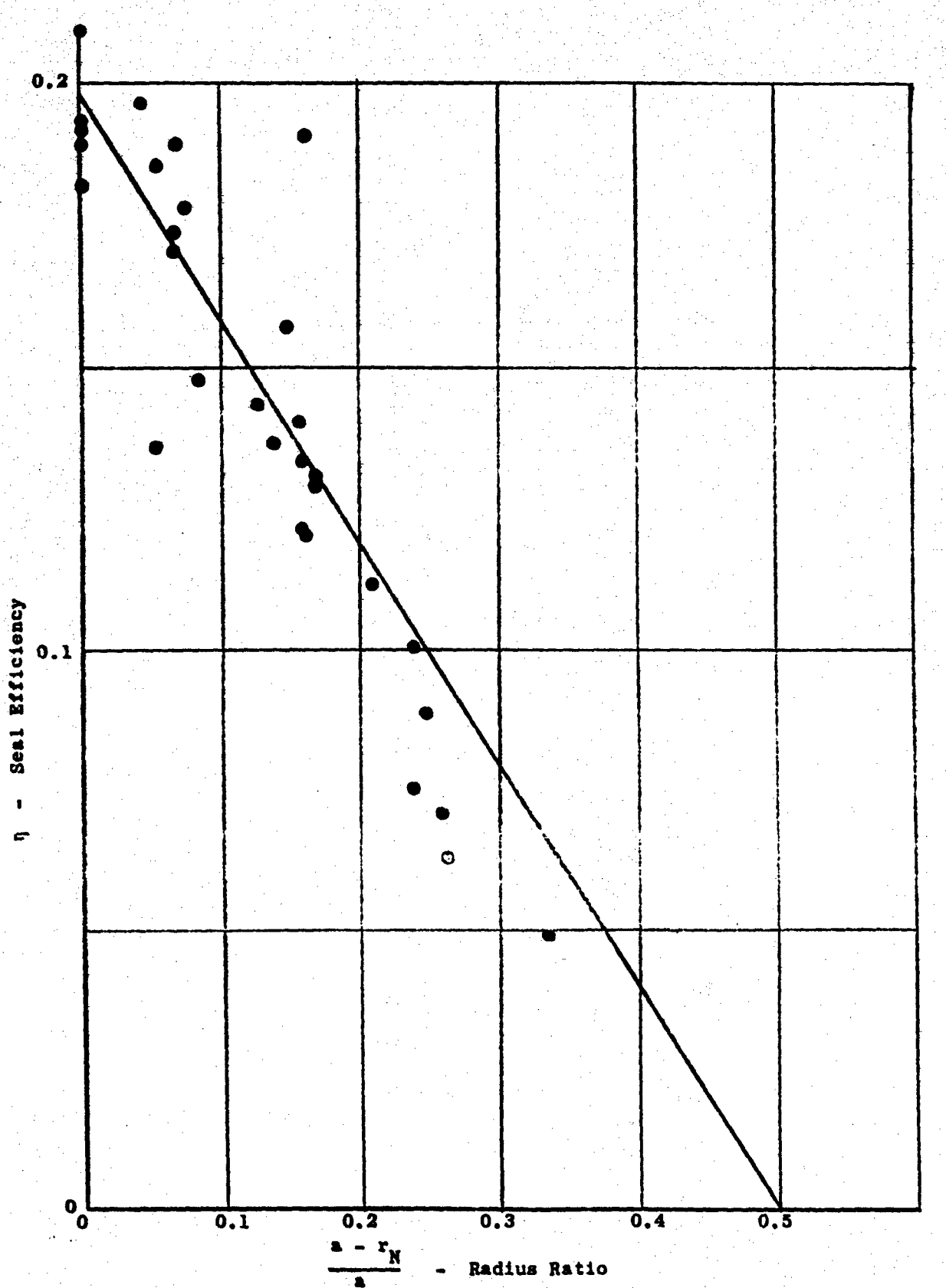

Figure 10b. Slinger Seal Efficiency, $\frac{rA}{a} = 0.52$, $\frac{SA}{a} = 0.092$.

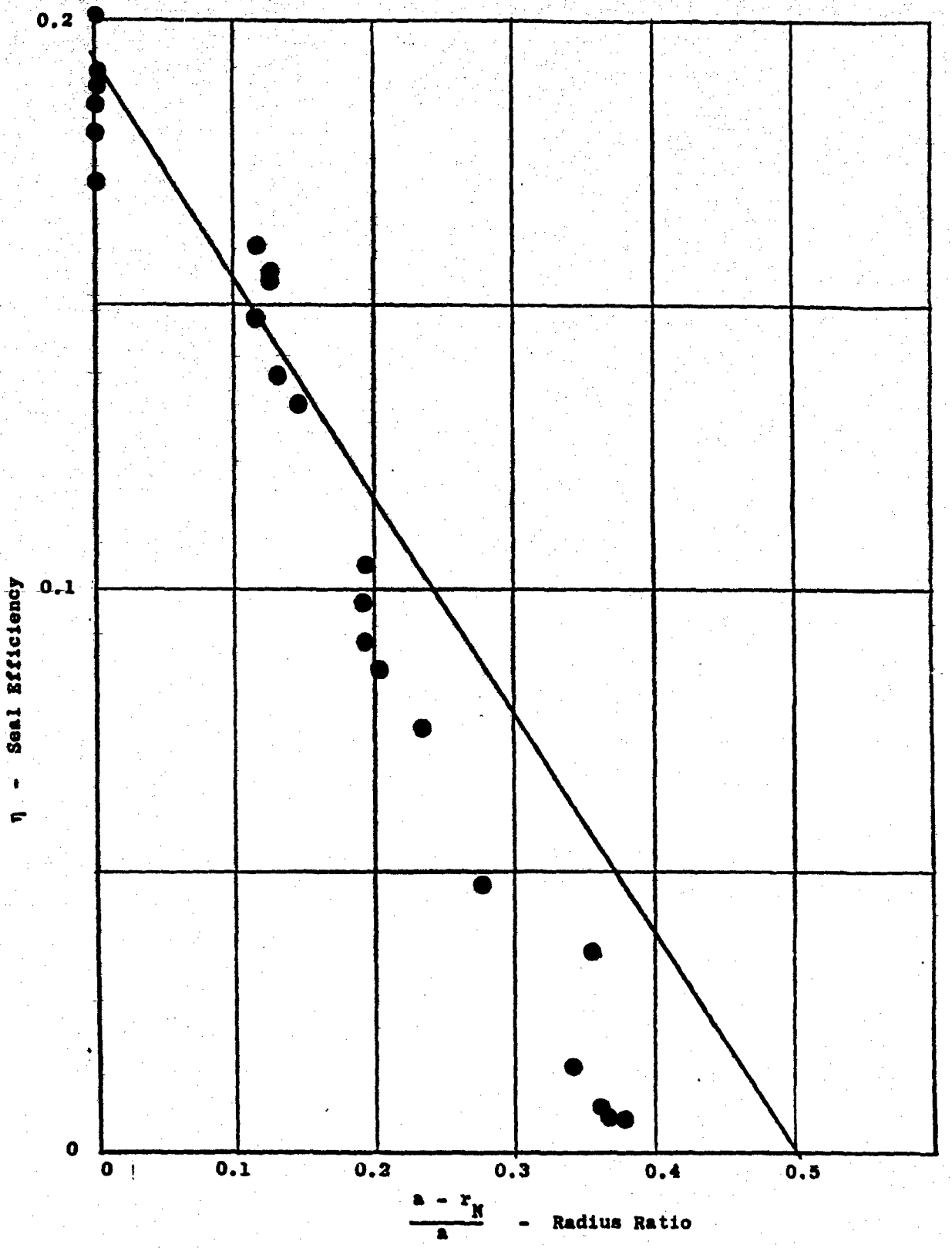

Figure 10c. Slinger Seal Efficiency, $\frac{rA}{a} = 0.52$, $\frac{SA}{a} = 0.019$

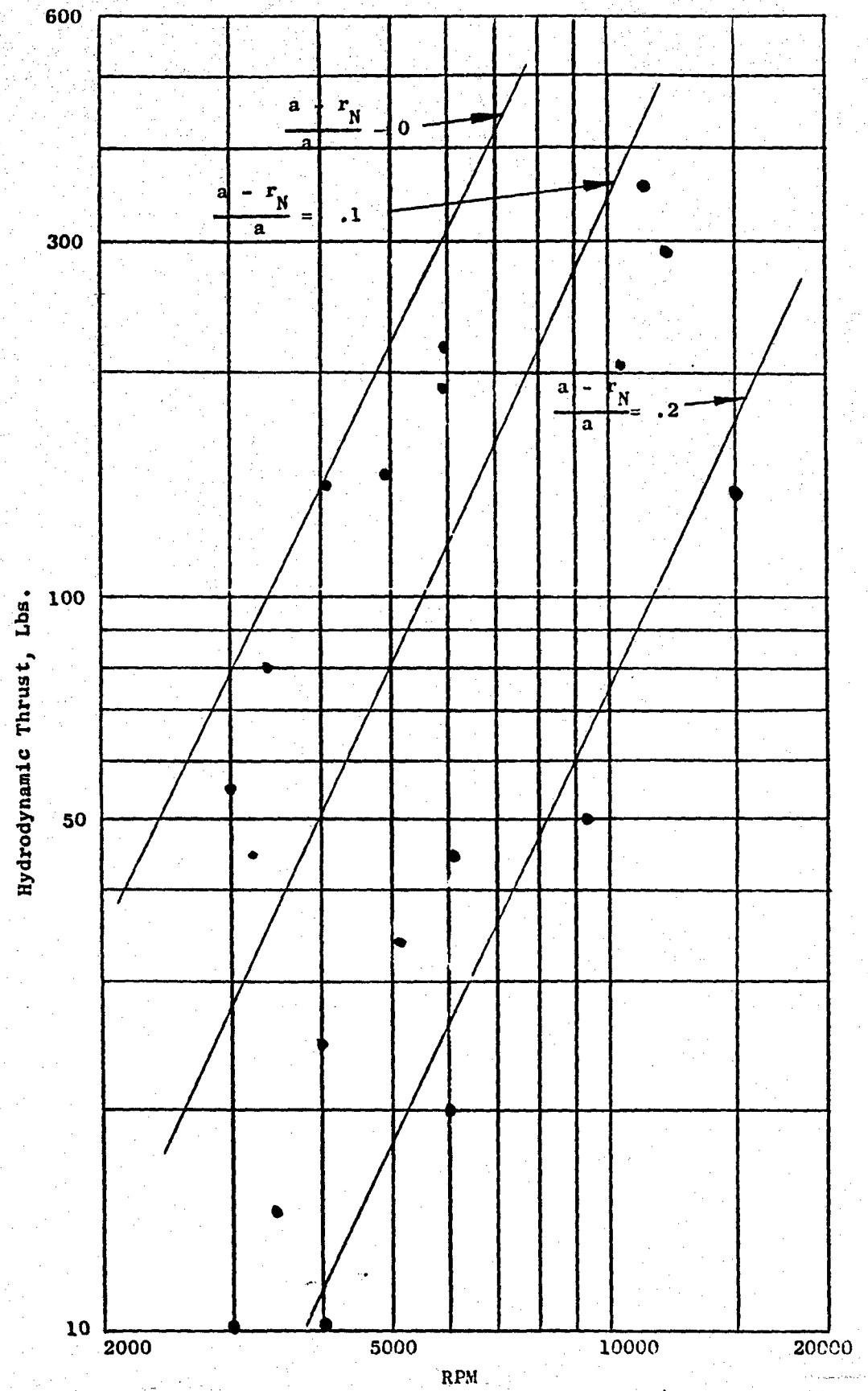

Figure 11a. Slinger Seal Hydrodynamic Thrust, $\frac{rA}{a} = 0.52$, $\frac{SA}{a} = 0.167$

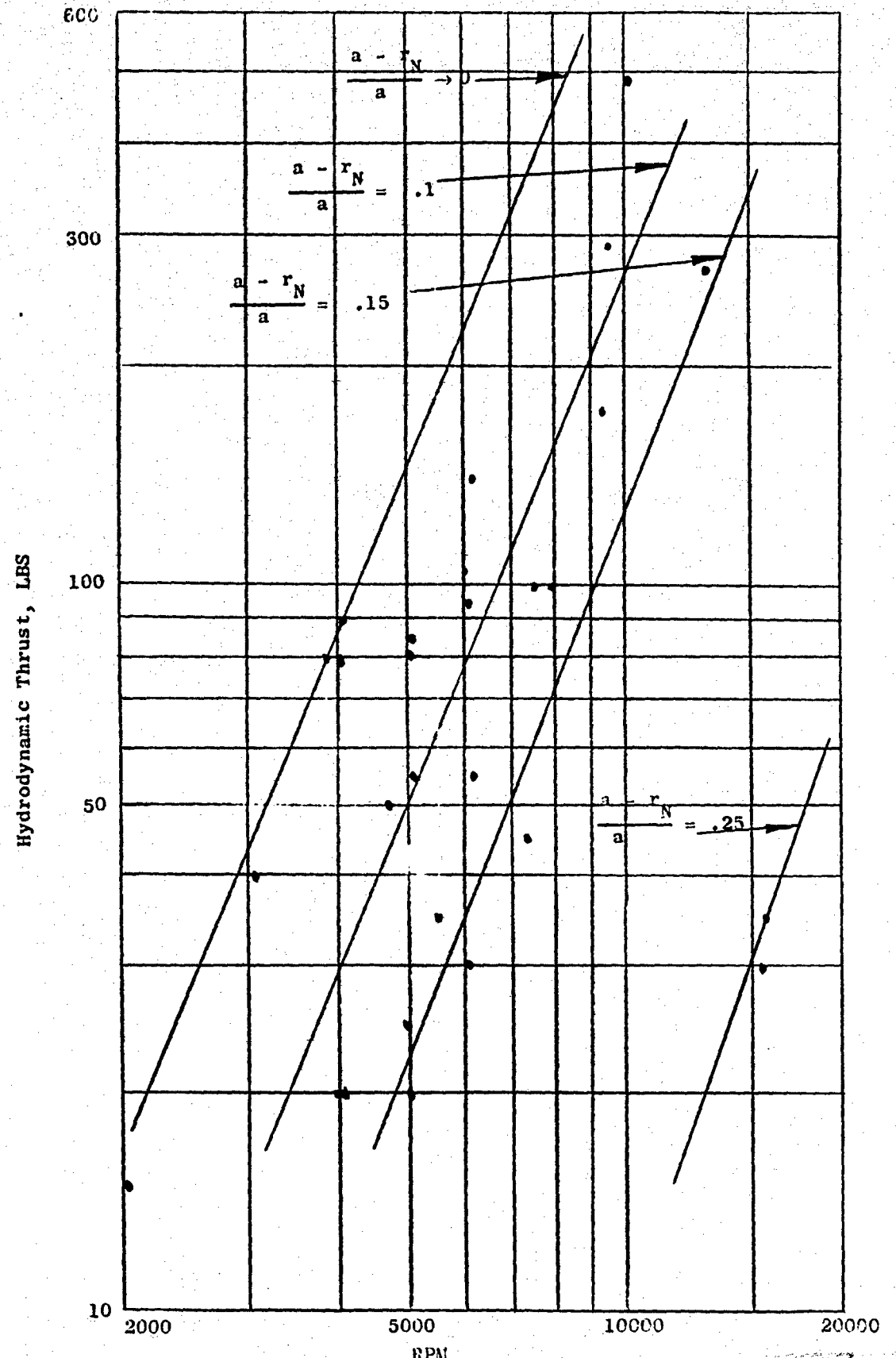

Figure 11b. Slinger Seal Hydrodynamic Thrust, $\frac{rA}{a} = 0.52$, $\frac{SA}{a} = 0.092$.

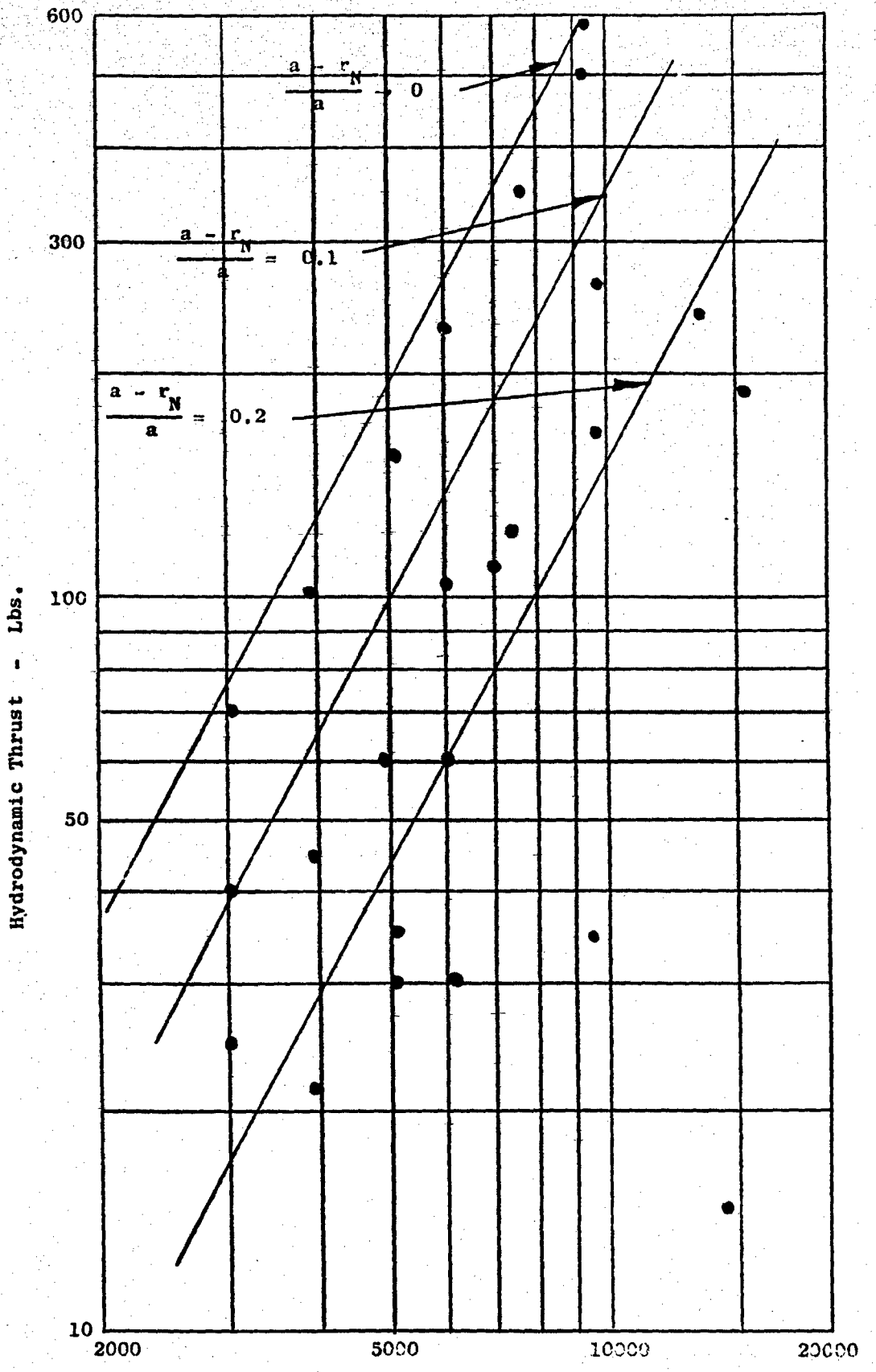

Figure 11c. Slinger Seal Hydrodynamic Thrust, $\frac{rA}{a} = 0.52$, $\frac{SA}{a} = 0.019$.

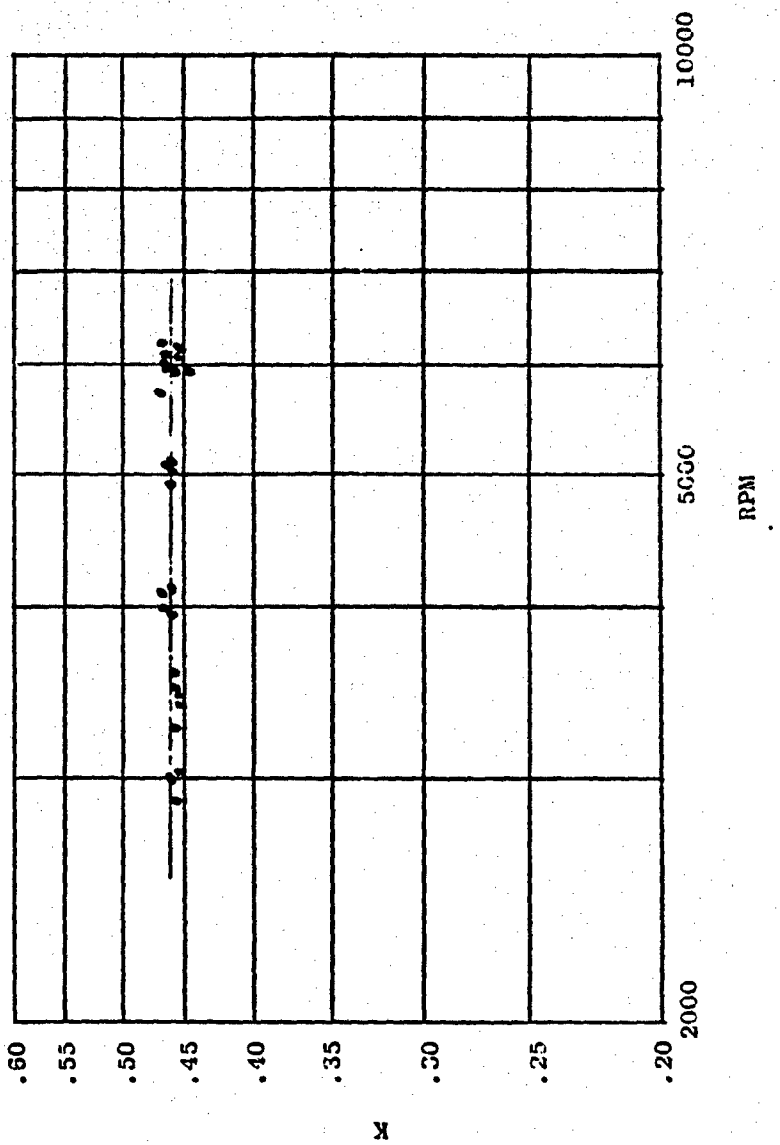

Figure 12a. Slinger Seal Velocity, $\frac{rA}{a} = 0.52$, $\frac{SA}{a} = 0.167$.

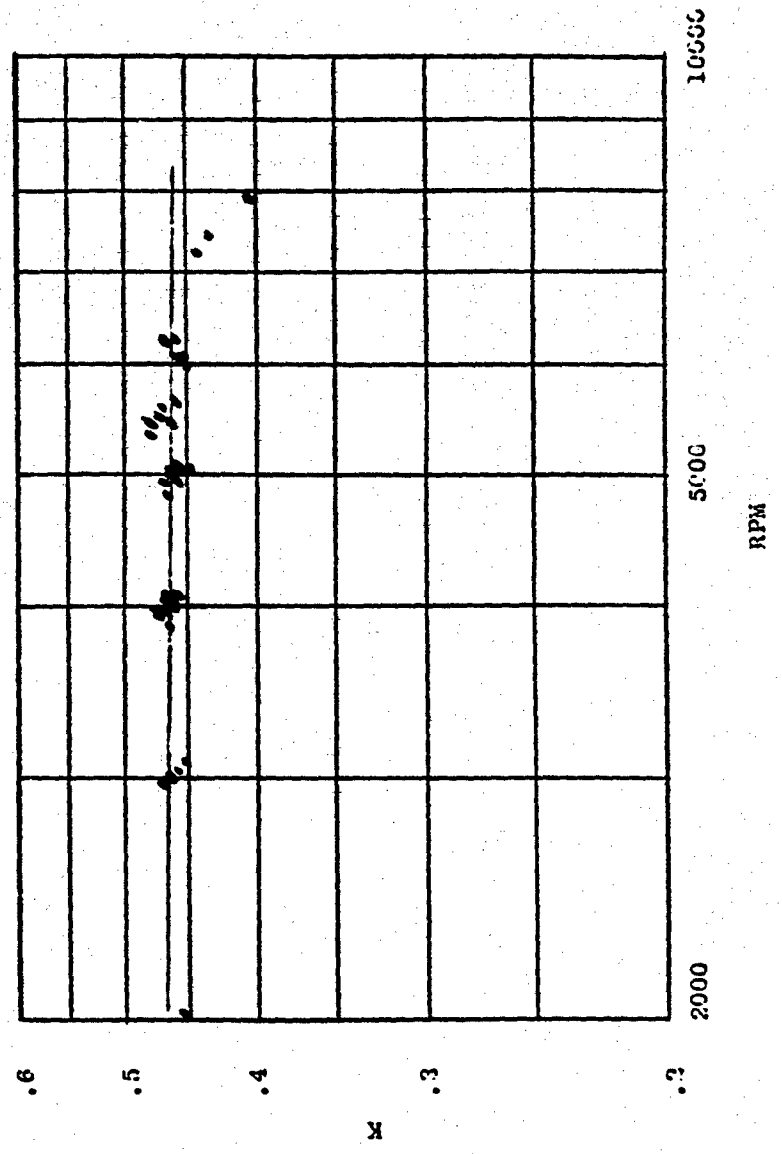

Figure 12b. Slinger Seal Velocity, $\frac{rA}{a} = 0.52$, $\frac{SA}{a} = 0.092$.

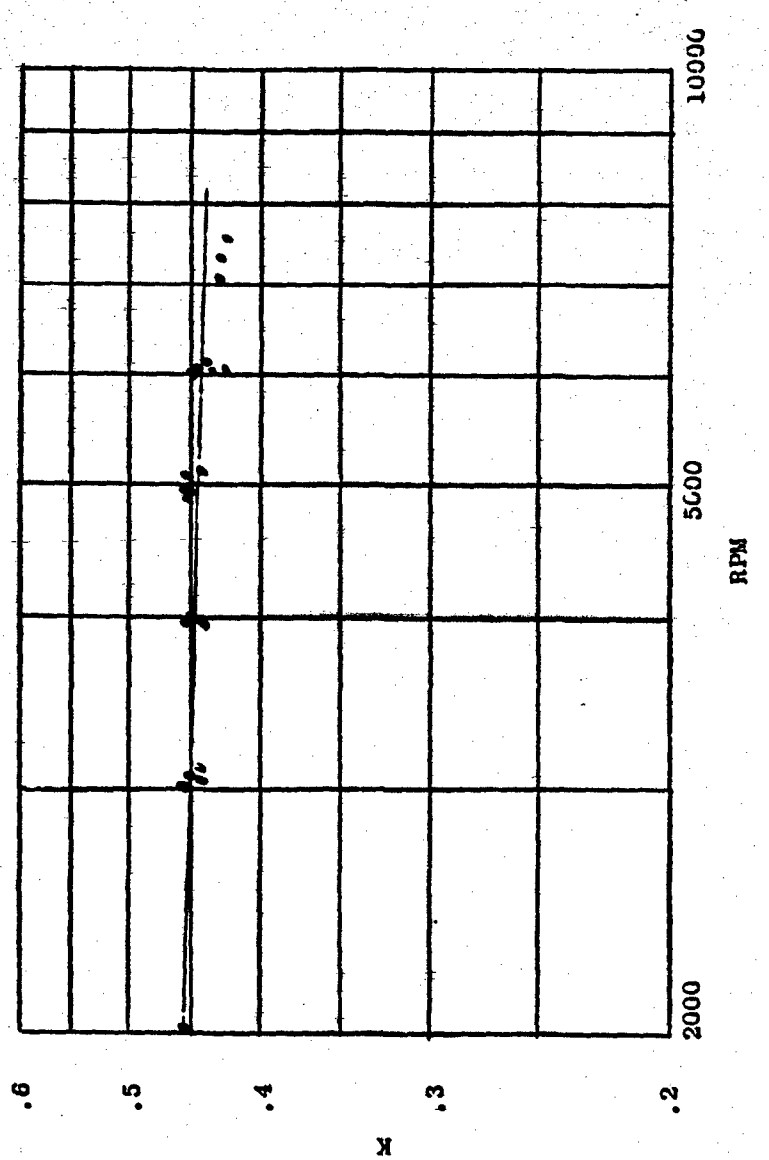

Figure 12c. Slinger Seal Velocity, $\frac{rA}{a} = 0.52$, $\frac{SA}{a} = 0.019$.

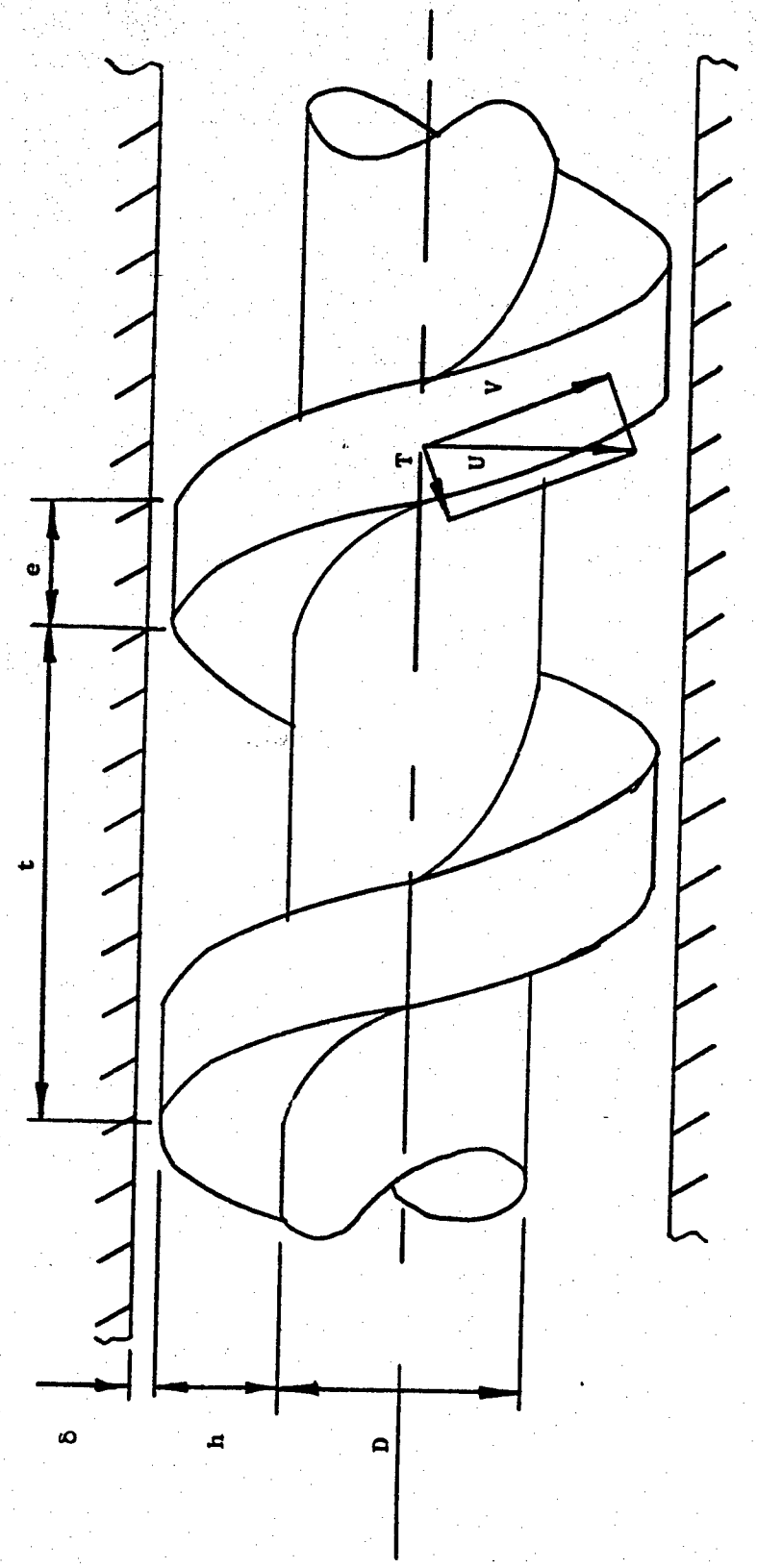

Figure 13. Screw Pump Diagram

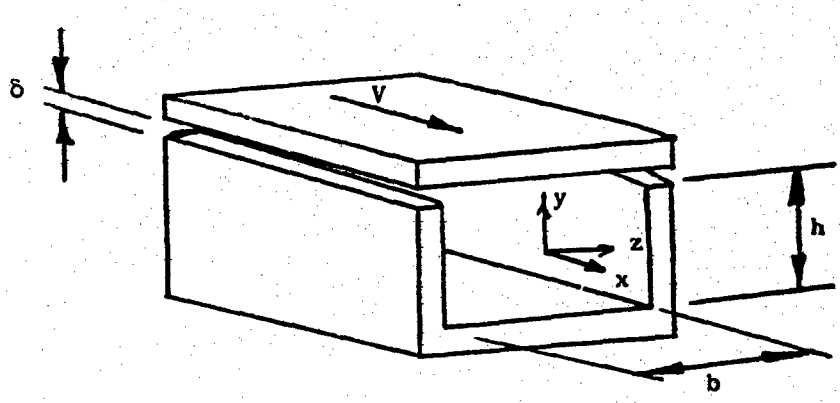

Figure 14a. Section of Screw Pump Channel.

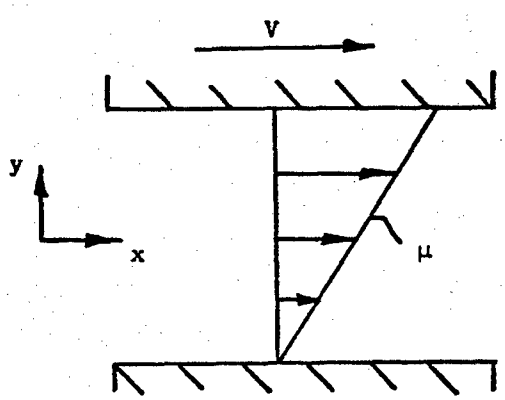

Figure 14b. Couette Flow Approximation in Screw Pump Channel.

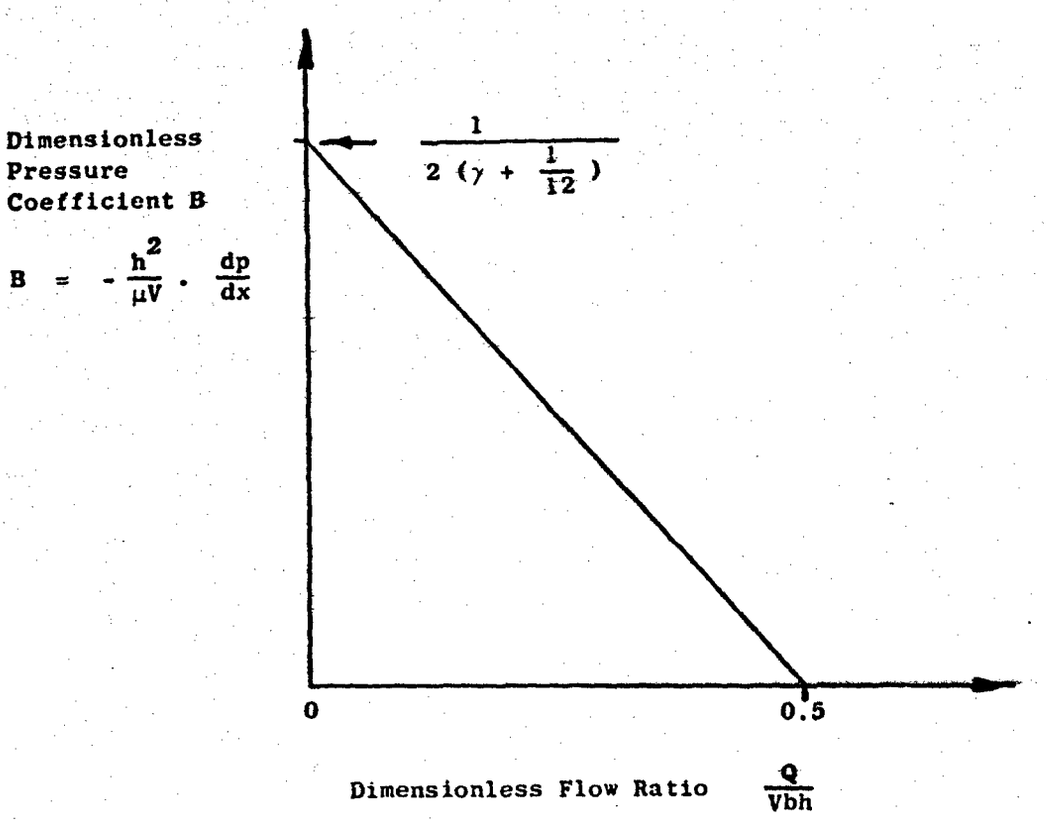

Figure 15. Screw Pump Characteristic with Laminar Flow.

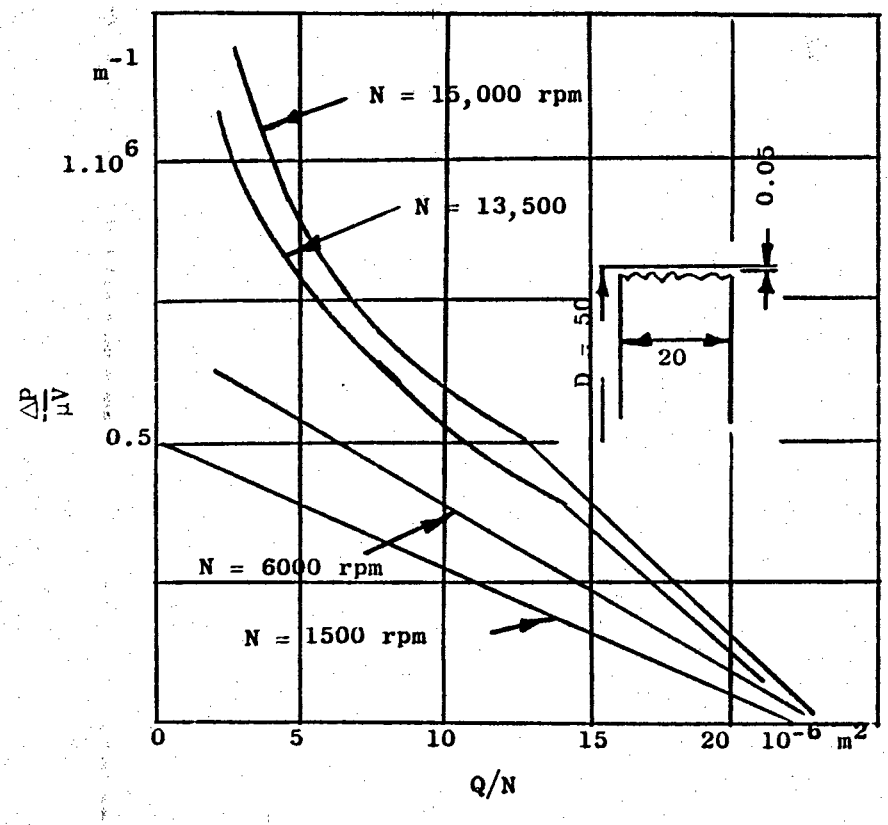

Figure 16

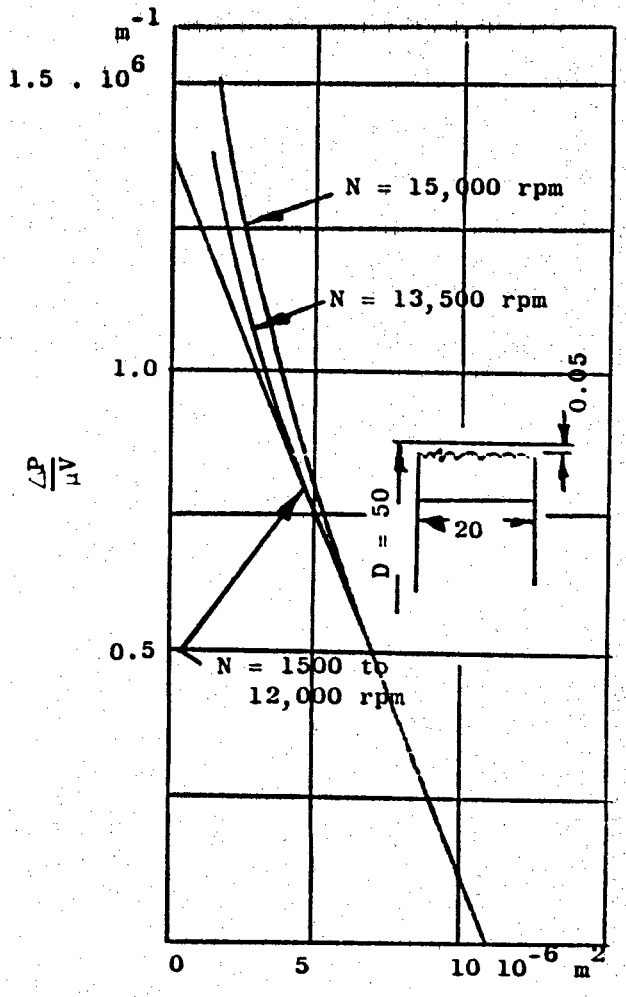

Figure 17

Screw Pump Pressure Characteristics

Typical Data of Frossel (Reference 4)

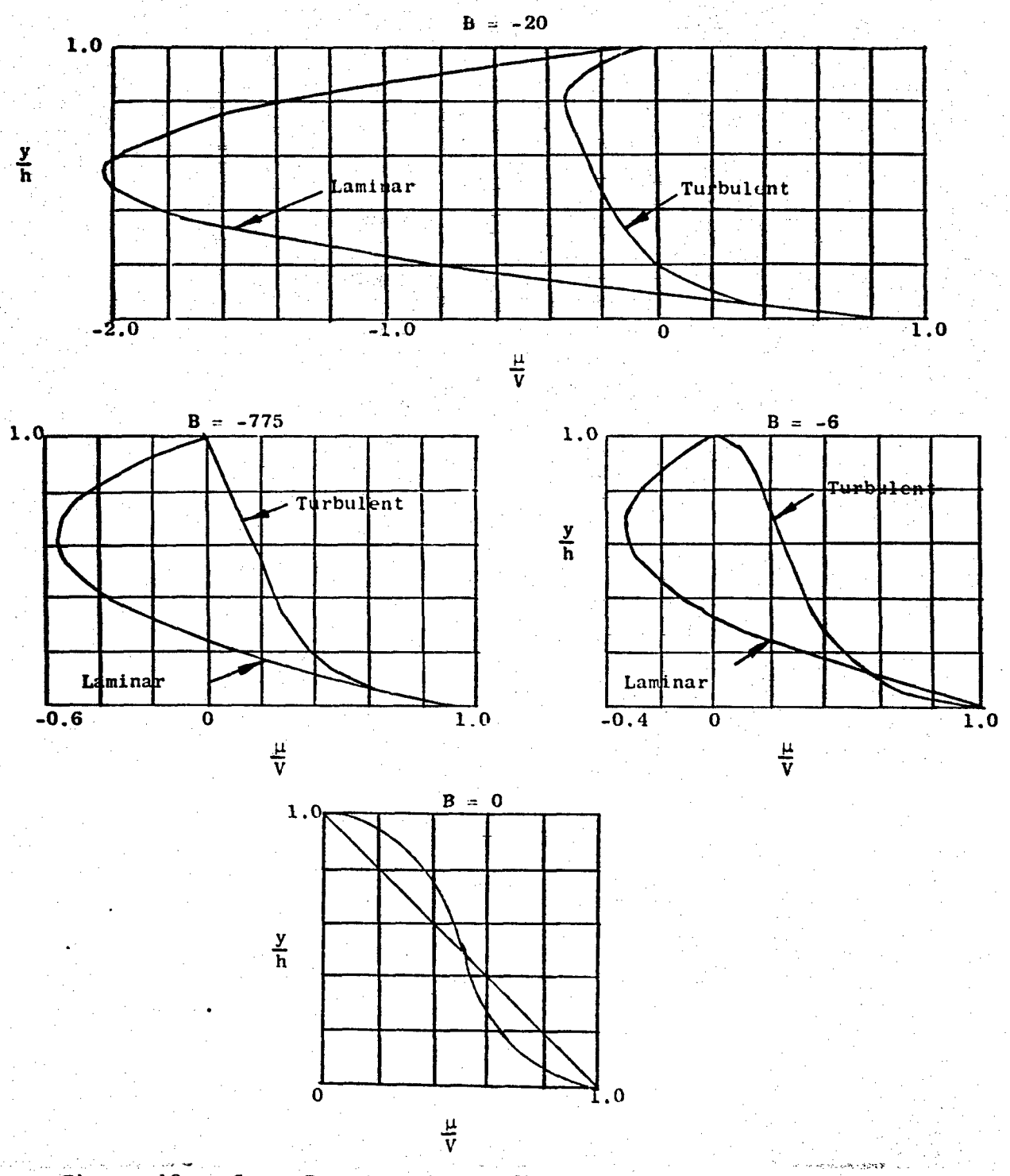

Figure 18. Screw Pump Velocity Profiles.

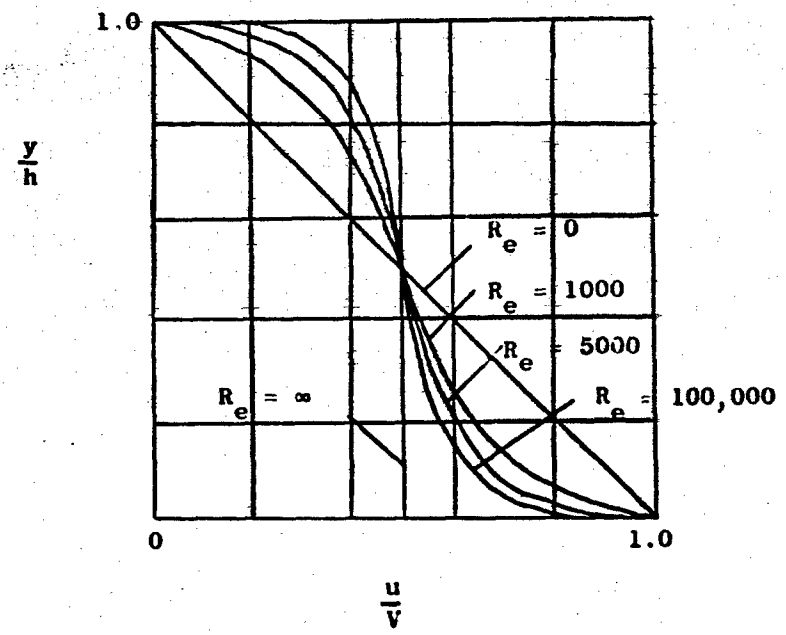

From Reference 5

Figure 19. Screw Pump Velocity Profiles with Couette Flow.

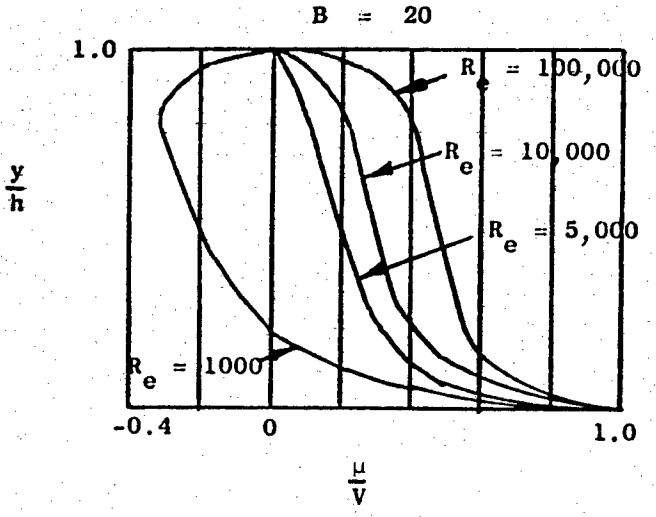

From Reference 5

Figure 20. Screw Pump Velocity Profiles.

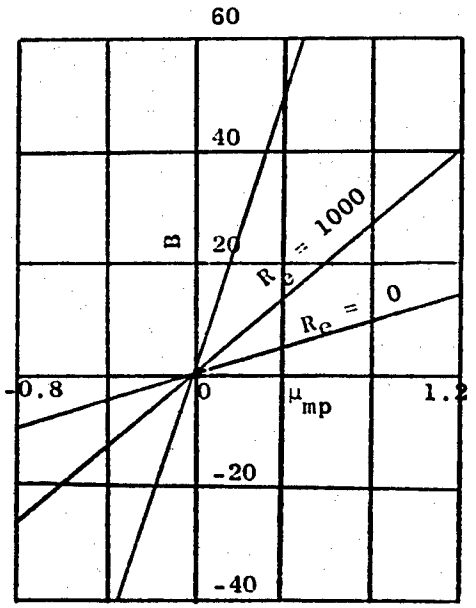

Figure 21. Screw Pump Pressure Coefficient.

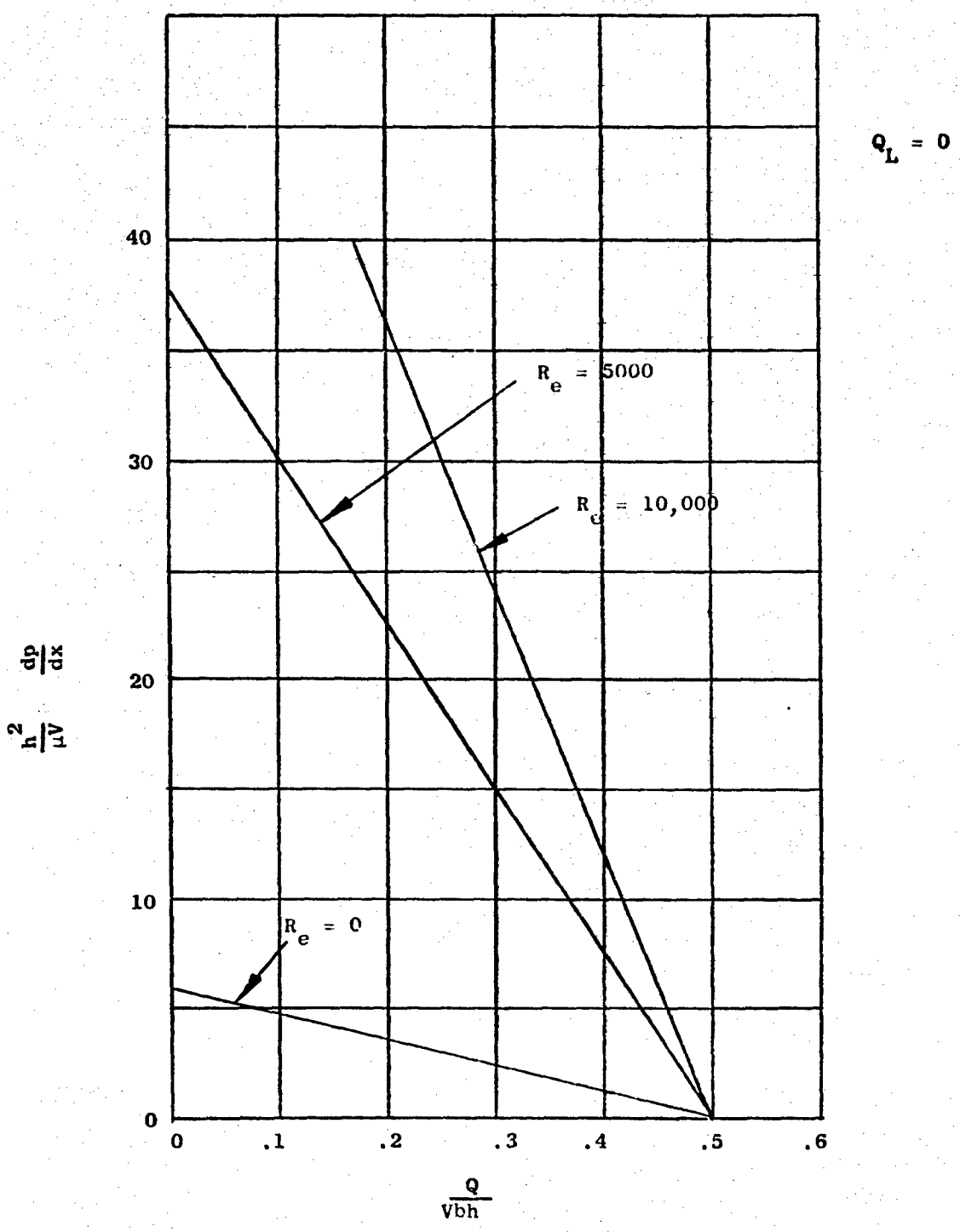

Figure 22. Screw Pump Theoretical Characteristics.

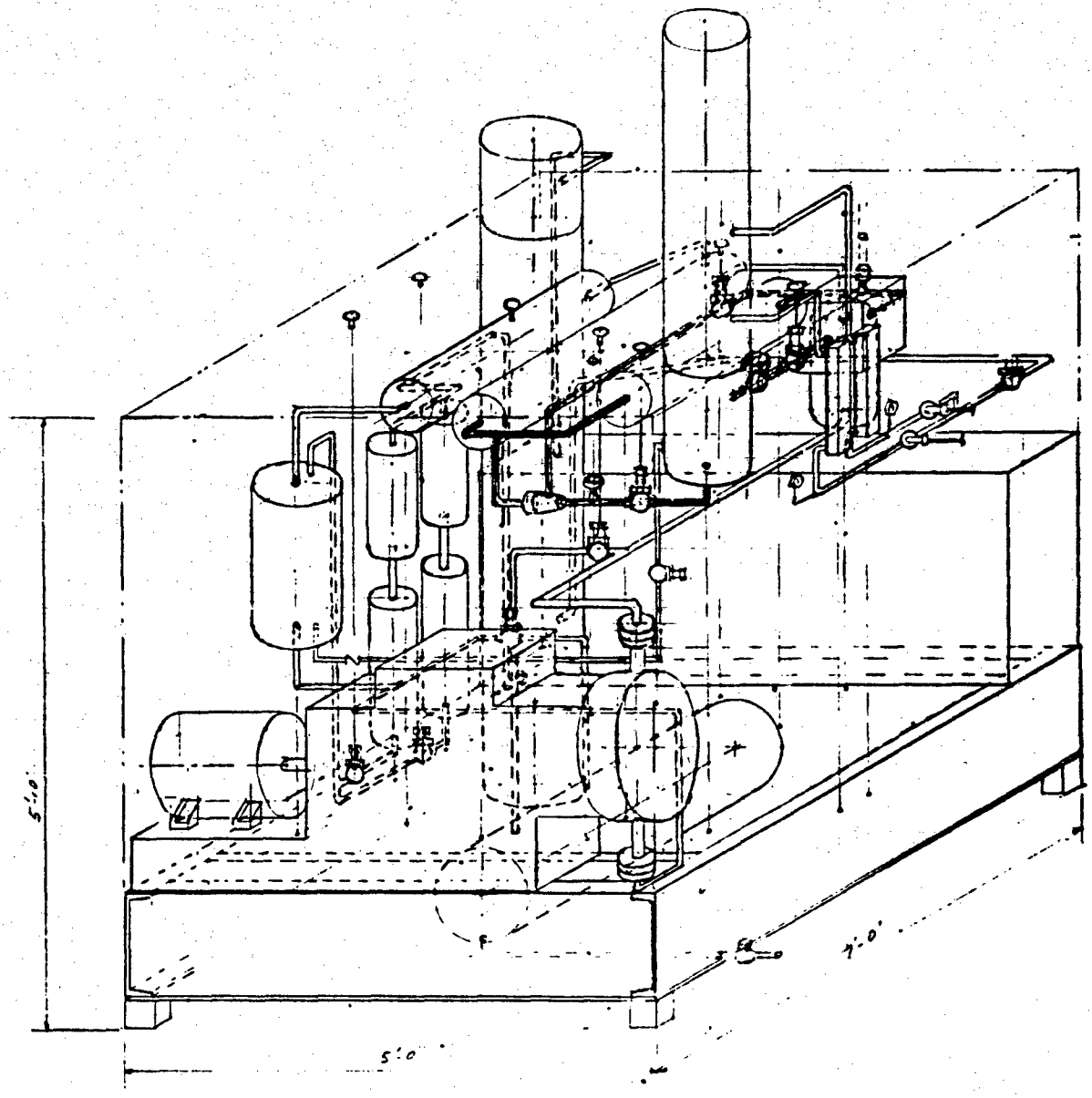

Figure 23. Alkali-Metal Dynamic Seal Test Facility Preliminary Layout Drawing.

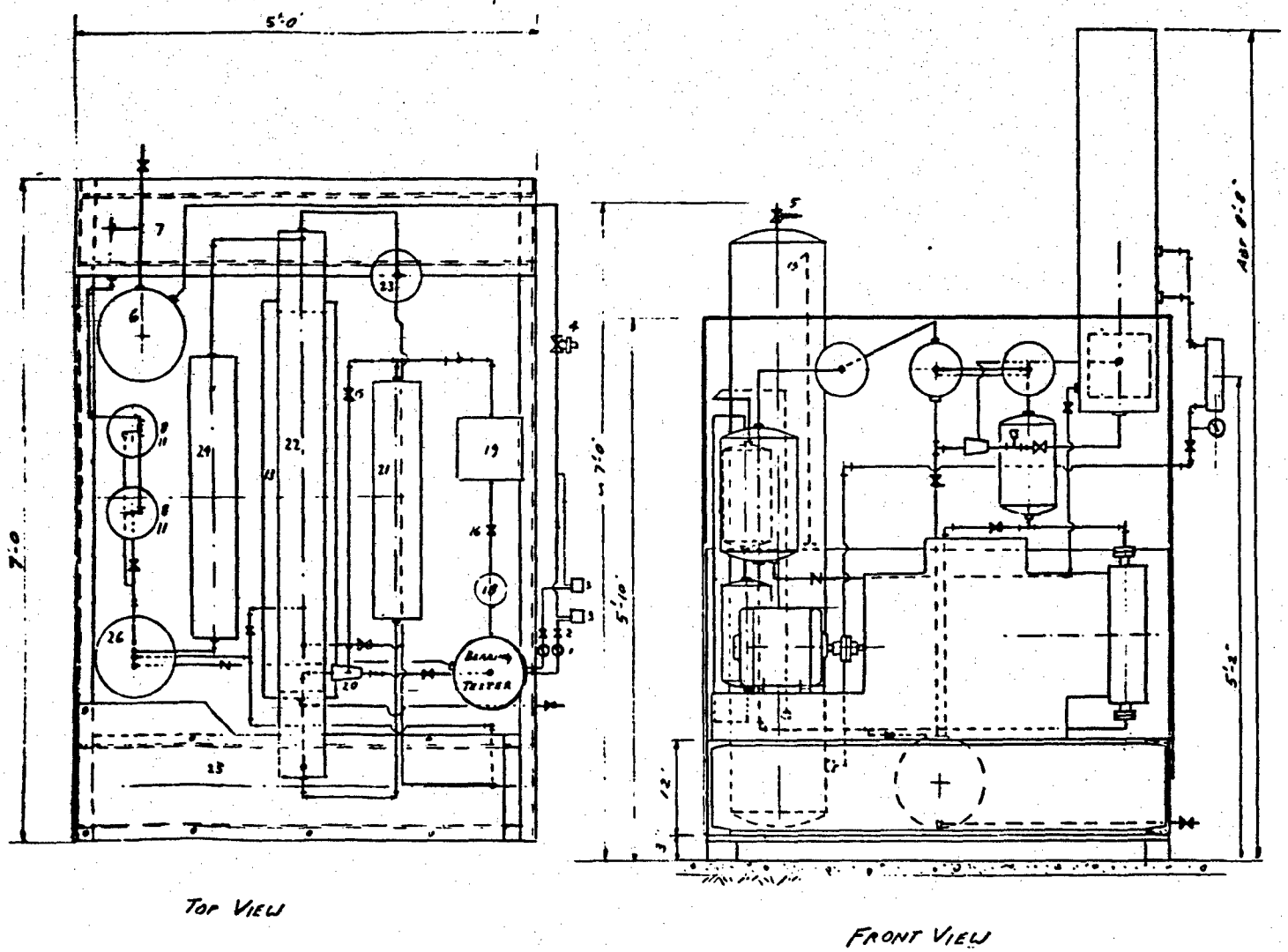

1

Figure 24. Alkali Metal Dynamic Seal Test Facility Prel
Isometric Drawing

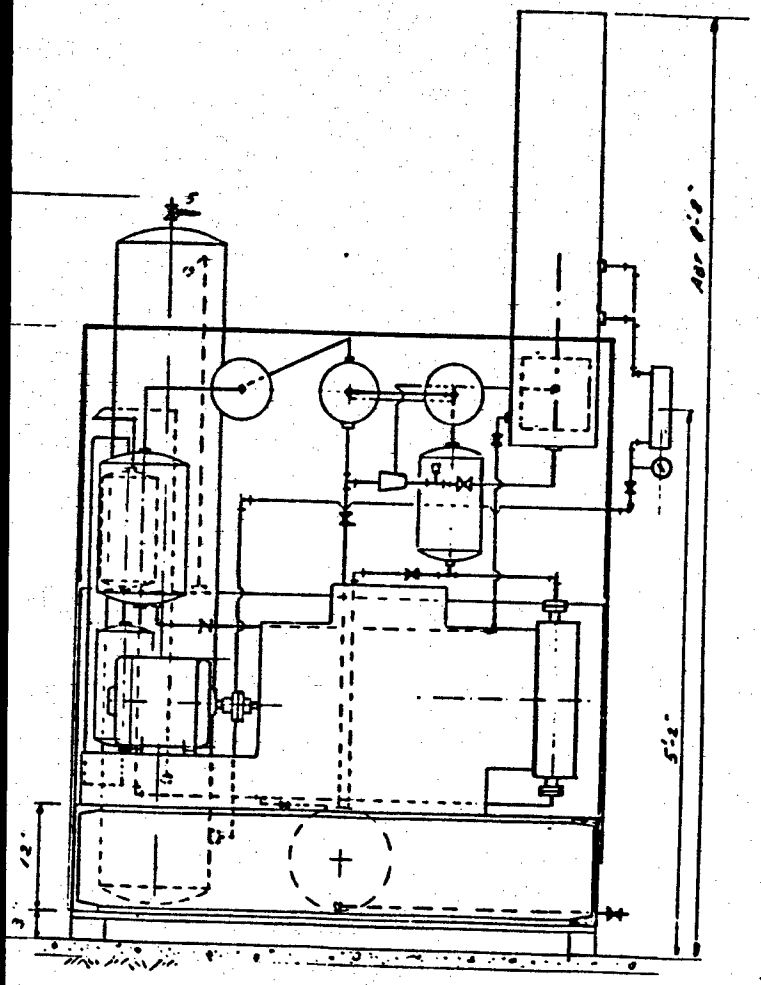

FRONT VIEW

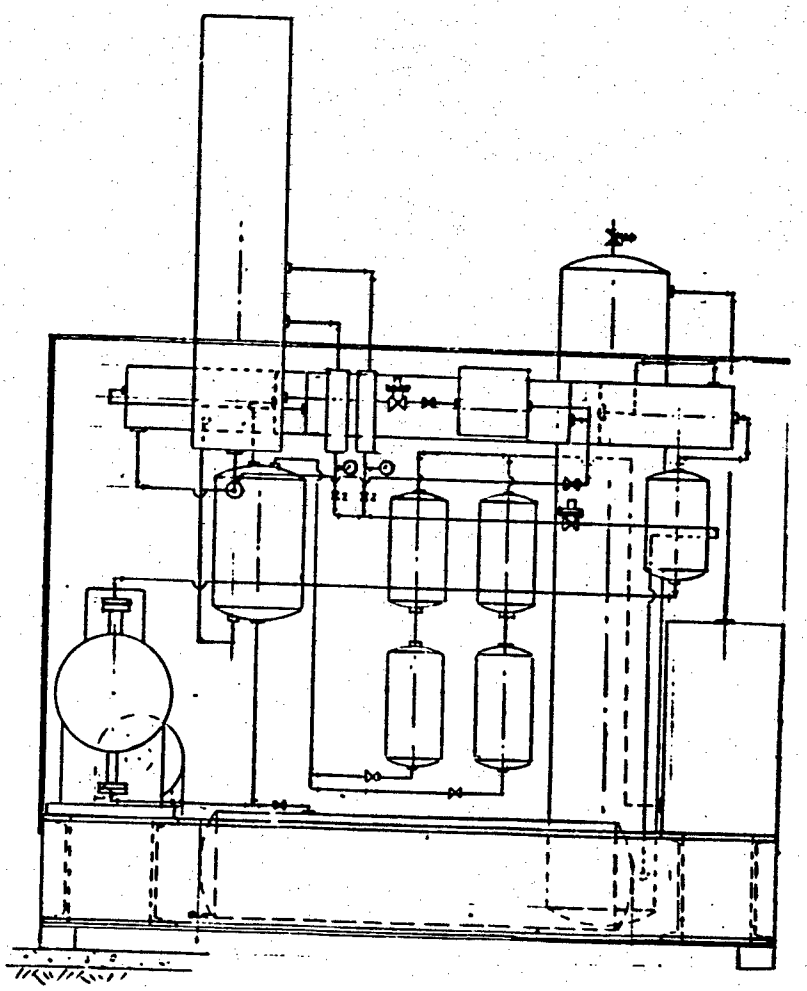

SIDE VIEW

24. Alkali Metal Dynamic Seal Test Facility Preliminary Isometric Drawing

2

Figure 24a

Item No.	Quantity	Item
1	2	Argon pressure gage
2	5	Sealed argon valve
3	2	Flowrater
4	1	Pressure regulator
5	1	Argon receiver
6	1	Pressure relief
7	1	Argon compressor
8	2	Micro filters
9	1	Argon heater
10	1	Motor blower
11	2	Cold traps
12	1	Dump tank
13	1	Insert
14	2	Level probes
15	2	Diaphragm valves
16	4	Globe valves
17	1	Check valve
18	1	L. M. Flowmeter

Figure 24a (contd)

Item No.	Quantity	Item
19	1	E. M. Flowmeter
20	1	Ejector
21	1	Cooler-Heater
22	1	Heat exchanger
23	1	Filter
24	1	Cooler and Valve
25	1	Pump
26	1	Head tank

DISTRIBUTION LIST

Copies	Organization
1	ASD (ASRCNC-2, Mr. John Morris) Wright-Patterson AFB, Ohio
1	ASD (ASRCTB-3, Mr. R. Ling) Wright-Patterson AFB, Ohio
1	ASD (ASRCNL, Mr. G. A. Beane) Wright-Patterson AFB, Ohio
1	ASD (ASRCMTP-3, Mr. R. J. Smith) Wright-Patterson AFB, Ohio
1	U. S. Atomic Energy Commission Office of Technical Information P. O. Box 62 Oak Ridge, Tennessee
1	Thompson-Ramo Wooldridge Attn: Mr. Carl Nau 23555 Euclid Avenue Cleveland 17, Ohio
1	Rocketdyne Division North American Aviation Attn: Mr. R. B. Dillaway Department 584 6633 Canoga Park Boulevard Canoga Park, California
1	Technical Information Center Aerospace Corporation P. O. Box 95085 Los Angeles 45, California
5	ASTIA Arlington Hall Station Arlington 12, Virginia

1	SSD (SSTRE, Capt. W. W. Hoover) AF Unit Post Office Los Angeles 45, California
1	Power Information Center Moore School Building 200 South 33rd Street Philadelphia 4, Pennsylvania
1	National Aeronautics and Space Administration Lewis Research Center Attn: Mr. Joseph Joyce Space Electric Power Office 25000 Brookpark Road Cleveland 35, Ohio
1	AiResearch Manufacturing Company Attn: Mr. John Dennan 402 - 536th Street Phoenix 34, Arizona
1	Sundstrand Aviation Corporation Attn: Mr. K. Nichols 2480 West 70 Denver 21, Colorado
1	Aerojet-General Nucleonics Attn: Mr. Paul Wood Azusa, California